EXPERIMENTAL INVESTIGATIONS OF VORTEX INDUCED VIBRATION OF A FLAT PLATE IN PITCH OSCILLATION

A Thesis

by

YI YANG

Submitted to the Office of Graduate Studies of
Texas A&M University
in partial fulfillment of the requirements for the degree of

MASTER OF SCIENCE

December 2010

Major Subject: Civil Engineering

EXPERIMENTAL INVESTIGATIONS OF VORTEX INDUCED VIBRATION OF A FLAT PLATE IN PITCH OSCILLATION

A Thesis

by

YI YANG

Submitted to the Office of Graduate Studies of
Texas A&M University
in partial fulfillment of the requirements for the degree of

MASTER OF SCIENCE

Approved by:

Co-Chairs of Committee,	Thomas W. Strganac
	Luciana R. Barroso
Committee Members,	John Niedzwecki
	Edward White
Head of Department,	John Niedzwecki

December 2010

Major Subject: Civil Engineering

ABSTRACT

Experimental Investigations of Vortex Induced Vibration of A Flat Plate in Pitch Oscillation. (December 2010)

Yi Yang, B.S, Chang'an University, China

Co–Chairs of Advisory Committee: Dr. Thomas W. Strganac
Dr. Luciana R. Barroso

A bluff structure placed in a flowing fluid, may be subjected to vortex-induced vibrations (VIV). For a flat plate with only rotational degree of freedom, the VIV is rotational oscillation. Based on the experimental investigation, vortex-induced oscillation of the plate is studied. The Strouhal number is measured from the stationary plate in a low speed steady wind tunnel. A set of vibration tests are conducted to investigate the relationships between shedding frequency and vibration frequency. "lock-in" phenomena is observed with and without large amplitude. An empirical-analytical model via introducing a nonlinear van der Pol oscillator is developed.

This thesis investigates the "lock-in" phenomena of a flat plate in pitch oscillation. Results from wind tunnel experiments on a flat plate indicate the "lock-in" is frequency "lock-in", resonance which appears large response amplitude occurs in the "lock-in" regime and may be influenced by "lock-in" phenomena.

To My Mother, Who Raised Me Up

ACKNOWLEDGMENTS

I would like to express my deepest appreciation and gratitude to my thesis advisor Dr. Thomas W. Strganac. For his guidance and warm-hearted encouragement during the course of this investigation. I also wish to thank my general advisor Dr. Luciana R. Barroso who excited my interest in structural dynamics and gave me a free space to do my research with Dr. Strganac. The financial support received through Vestas Wind Energy is gratefully acknowledged.

I wish to extend my appreciation to my good friends David MacKenzie, Nick Colson, R.J. Brey and Hong Zhang in Civil Engineering Department, who helped me in my study when I came to Texas A&M for the first year. My thanks is also extended to Department of Aerospace Engineering with whom I have worked, Dr. Celine D. Kluzek, Shalom Johnson and Yogesh Babbar. I also would like to thank all my committee members, Dr. Niedzwecki who gave me an insightful introduction in fluid-structure interaction in the course I took, and Dr. White who gave me suggestions on aerodynamics and wind tunnel test.

Lastly, and most importantly, I thank my parents and other family members, for their support and encouragement. Thanks also been extend to my good friends Xu Han, Jialiang Wang, Yichuan Peng and Zhen Zheng who spent time with me and encouraged me through the difficult moment in the course of my graduate work.

TABLE OF CONTENTS

CHAPTER Page

LIST OF TABLES

LIST OF FIGURES

FIGURE Page

CHAPTER I

INTRODUCTION

A bluff structure placed in a flowing fluid may be subjected to vortex-induced vibration (VIV). The phenomenon can occur with both bluff bodies and streamlined bodies, and has been observed in numerous fields such as aerospace engineering, civil engineering, mechanical engineering and ocean engineering. In the field of structural engineering, these oscillation are of great interest not only because of the large response amplitude which might over-stress a structural member but also because of the long term cyclic loads which may cause failure by fatigue. Recently, with the renewed interest of wind energy systems, oscillations of wind turbine blade attracts attention. It has been observed that there is a large vibration amplitude of wind turbine blades on the wind farm site, and been considered as VIV problem. This research investigates the rotational response of a flat plate in the wind tunnel to provide a basic view of VIV in pitch oscillation.

A. Basic Phenomena of VIV

In the area of VIV research, an oscillating circular cylinder is a classical problem. The oscillating forces induced by vortex shedding are created by the fluctuation of fluid pressure on the structure's surface. The fluid pressure fluctuates as vortices are shed alternately from each side of the structure. Vortex shedding generates a periodic asymmetric flow which is well known as the Karman vortex street.

The journal model is *Journal of Fluids and Structures*.

Vortex shedding regimes from a fixed circular cylinder vary with flow velocities. For the low flow velocities (Reynolds number as low as $Re < 5$), the flow around cylinder still remains unseparated. When $Re > 5$ *or* $15 < Re < 40$, a fixed pair of vortices in wake is generated. For $40 < Re < 90$, vortex street is laminar. Transition range in which vortices translate from laminar flow to turbulent flow has been observed at $150 < Re < 300$. From $Re > 300$ to $Re < 3 \times 10^5$, vortex street is fully turbulent. In the range of $3 \times 10^5 < Re < 3.5 \times 10^6$, the laminar boundary layer has undergone transition to turbulent flow, and wake is narrow and disorganized. When $Re \geq 3.5 \times 10^6$, a turbulent vortex street would be re-established.

The frequency of vortex shedding has a possible relationship with the flow velocity. This relationship is characterized by the Strouhal number

$$S_t = \frac{f_{st} D}{V} \tag{1.1}$$

where f_{st} is the frequency of a complete cycle of vortex shedding for the body at rest (also referred to as Strouhal frequency). D is a characteristic structure dimension perpendicular to the direction of flow. V is the velocity of coming flow. The Strouhal number of a stationary cylinder in a subsonic flow is a function of Reynolds number, surface roughness and free stream turbulence.

The alternated shedding of vortices causes oscillating lift and drag forces on the circular cylinder. The response to the oscillating lift force may be vibration in a direction transverse to the flow, if the cylinder is free to move. These type of vibrations are referred as "Vortex-induced Vibration"(VIV).

For structures at rest, vortices shed at the shedding frequency which is the

Strouhal frequency(f_{st}). For sufficiently small amplitudes of structural oscillation, the vortex sheds in a undisturbed process. In this case, the vortex shedding frequency (f_{vs}) equals to the Strouhal frequency and the response frequency of the system is also at the Strouhal frequency. However, as the flow velocity increases or decreases so that the shedding frequency is in the neighborhood of the natural frequency of the structure, vortex shedding frequency suddenly lock into the natural frequency of structure. This phenomenon is a critical condition in VIV, also called "lock-in" or synchronization.

The early studies found that "lock-in" occurs when the flow velocity is such that $f_{st} \approx f_{ex}$, and then the actual vortex shedding frequency is close to the excitation frequency, $f_{vs} \approx f_{ex}$. It is characterized by a certain sudden and significant response in aeroelastic excitation mechanism. Later studies corrected the definition and found there is a bandwidth of "lock-in" frequencies. "Lock-in" may be found in the bandwidth even if in the velocity is such that $f_{st} \neq f_{ex}$. The significant increase in the length of vortices causes a large increase in the corresponding force along the structure. Distinguished from classical resonance, the "lock-in" mechanism is self-limiting with a large amplitude.

"Lock-in" may lead to poor performance of structure and may also cause failure of structural members. The large response observed from "lock-in" may cause over-stressed problems. Even if there is no large amplitude observed, sustained vibration still may cause some long term problems, for example, fatigue of structural members. This thesis focuses on the "lock-in" phenomena of a flat plate in pitch oscillation. This may provide a basic view of rotational motion and torsional response of vortex induced vibration problems for a plate structure such as wind turbine blade.

B. Natural Wind Induced Vibration

Structural members such as wind turbine blades, flat steel box girders of long span bridges and top-side members of offshore platforms may be excited by vortex shedding. Both wind speed and direction of the natural wind may vary and there exists a critical wind velocity at which large amplitude of vibration may be observed.

Random fluctuations of wind velocity may cause random vibration of structural members. Although the amplitude of random vibrations may be smaller than that of steady-state vibration under the critical wind velocity, the response on the structure members from random vibration may cause fatigue problems which is difficult to be predicted due to aerodynamic and structural interaction.

For plate structure members such as wind turbine blades and flat steel box girds of long span bridges, three degrees of freedom (rotation, in-line and cross-line) may be affected as a result of vortex shedding. In aeroelasticity, rotational motion is referred to as pitch, in-line motion is referred to as plunge and cross-line motion is referred to as lead-leg. These three motions are coupled to each other in vibration by aerodynamic load and structural response. The coupled motions may also lead to instability problems. Torsion generated by pitch may induce large bending, while bending generated by plunge may induce large torsion. It is important to understand each mode of motion and their coupled effects. Cross-line is a well known motion in VIV of a circular cylinder. Many experimental and theoretical investigations have been done from previous research. Pitch oscillation is not observed for the oscillating cylinder.

However, it is observed for certain plate structures. Therefore, in this thesis, a plate system with pitch motion as a single degree of freedom system has been investigated in a low speed wind tunnel.

C. Outline of Investigation

This research is primarily experiment-based research aiming at investigating the fundamental phenomena and theories of vortex induced oscillating rotation of a flat plate. A group of tests, including both stationary and vibration tests about the flat plate, were conducted in a $2' \times 3'$ low speed wind tunnel in the Aero and Fluid Dynamic Lab at Texas A&M University. A preview of each chapters that follow are briefly summarized as below.

Chapter II is a critical review of work related to both theories and experiments which have been done by previous researchers. In Chapter III, a detailed description of the test apparatus and measurements of each test has been illustrated. Chapter IV opens with the measurement of the Strouhal number of the flat plate. Following this, flow passing the stationary plate has been pictured via flow visualization. After that a group of vibration tests which focus on "lock-in" phenomena, including the measurement of structural vibration frequency and vortex shedding frequency, is presented. An empirical-analytical SDOF mode has been developed by introducing the van der Pol nonlinear oscillator. Comparison with experiential results are given. In Chapter V, a short statement of the main conclusions obtained from both test results and analytical results are made. Recommendations for further work that are necessary to expand experiments and theories are given.

D. Glossary of Terms

This section provides several important concepts that are used in the thesis.

Aerodynamic Moment Coefficient (C_m)

A non-dimensional number, defined by $C_m = \frac{M}{1/2\rho V^2 Sc}$, where M is the aerodynamic moment about a certain point, ρ is the density of air, V is flow velocity, S is the area of plate, and C is the chord length of plate.

Damping Coefficient (c)

A coefficient qualifying damping effect of system. For this system, $M = c\dot{\theta}$, where M is the moment load and $\dot{\theta}$ is the angular speed of rotation ($\frac{kg \cdot m^2}{s}$).

Damping Ratio ζ

Defined as the ratio of damping coefficient to critical damping ($\zeta = \frac{c}{2I\omega_{vac}}$, where I is the mass moment of inertia).

Frequency in Air (f_{air})

Frequency of the structure measured in the air from a free vibration test (Hz).

Frequency in Vacuum (f_{vac})

Frequency of the structure measured in the vacuum from a free vibration test. It is also considered as theoretical natural frequency (Hz).

Reynolds Number (Re)

A dimensionless number that gives a measure of the ratio of inertial forces to viscous forces ($Re = \frac{\rho V D}{\mu}$, where μ is the dynamic viscosity of fluid).

Reduced Velocity (V_r)

A normalized flow velocity, defined by $V_r = \frac{V}{f_{vac} D}$, where D is the dimension of a bluff body. For the plate $D = C$ represents chord length of the plate.

Strouhal frequency f_{st}

Frequency of vortices shed from a stationary bluff body (Hz).

Strouhal Number (S_t)

A dimensionless number describing oscillating flow mechanisms,defined by $S_t = \frac{f_{st} D}{V}$.

Vibration Frequency (f_{ex})

Vibration frequency of the structure, also been referred to as excitation frequency (Hz).

Shedding Frequency (f_{vs})

Frequency of vortices shed from a vibrating bluff body (Hz).

Circular Frequency (ω)

Defined by $\omega = 2\pi f$, where f represents frequency. Circular frequency is the concept related to its corresponding frequency. For example, $\omega_{vac} = 2\pi f_{vac}$ represents circular natural frequency.

CHAPTER II

REVIEW OF PREVIOUS WORK: EXPERIMENTS AND THEORIES

This chapter opens with a discussion related to the phenomena of vortex-induced vibrations, especially for the bluff body under physical "lock-in" phenomena. A review of past and recent research including both experimental observations and theoretical models is given in this chapter. Since VIV phenomenon is primarily focused on the oscillating cylinder rather than plate structure, the common VIV mechanism and phenomena are discussed in this chapter.

A. Preliminary Remarks

From the years when the mechanism of vortex shedding and the structure of wakes were first investigated by *von Kármán*, the research on vortex induced vibration started to develop. *Von Kármán*'s analysis has been followed by numerous studies of vortices wakes, and the lift and drag forces in bodies with separating flows.

The early 1940's brought observations on the response of structures allowed to vibrate under the influence of vortex shedding forces. Ocean engineers placed emphasis on such observations. They observed vibrations of riser system or mooring lines of ocean platforms with large amplitude. This phenomenon caused fatigue problems, even leading to failure of the platforms. Later, structural engineers found similar phenomenon on wind turbine blades and girders of long span bridges under a certain range of wind speed.

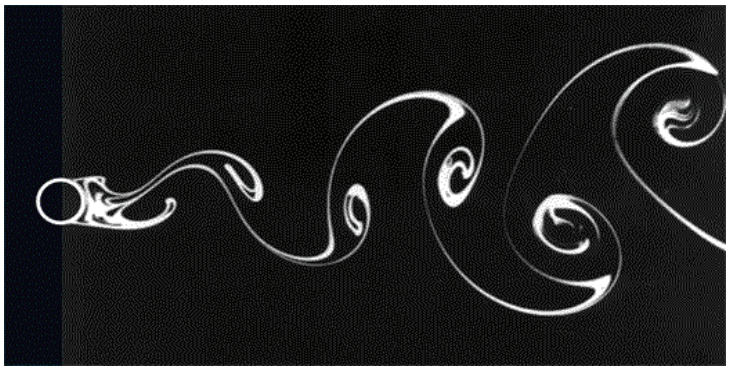

Fig. 1. *Kármán* Vortex Street (Van Dyke, M 1982)

When placed in a fluid (water or gas) flow, a bluff structure (also referred to as a bluff body) will lead to flow separation. The separation may change the flow field from steady flow to unsteady flow with an increase of the Reynolds number. At a low Reynolds number, the flow surrounding the body remains steady when flow separation first occurs. With increasing Reynolds number, at a certain value, instability in the shear layers of the separation flow will be developed. Therefore, a nonlinear interaction between these layers with feedback from the wake leads to a periodic and organized vortex street, which is known as the *Kármán* Vortex Street. The vortices are organized in two rows with opposite circulation. These numerous vortices constitute the characteristic of the downstream turbulence which has been observed in the flow visualization as shown in Figure 1.

A dimensionless number describing oscillating flow is called the Strouhal number (S_t), as named after Vincenc Strouhal. Strouhal reported that the vortex shedding which results from nonlinear interaction between two shear layers is affected by a feedback from the wake and shape of the structure body. The Strouhal number is

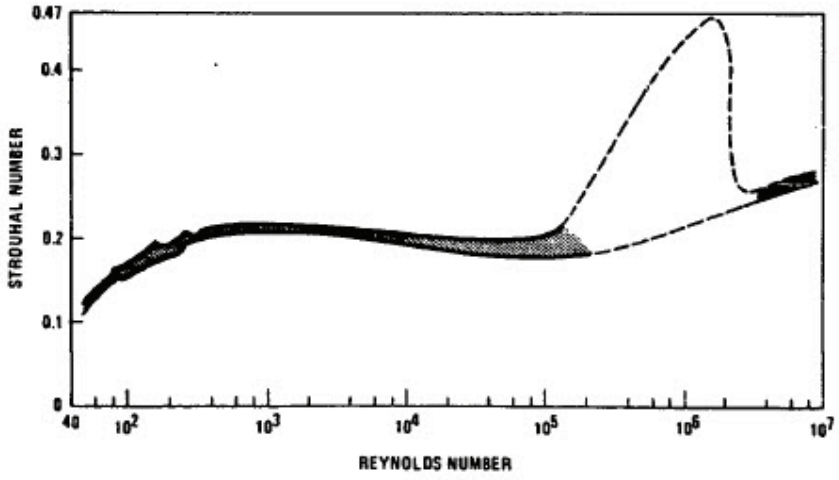

Fig. 2. S_t versus Re (Blevins 1977)

defined as

$$S_t = \frac{f_{st} D}{V} \tag{2.1}$$

where f_{st} is frequency of one complete cycle of vortex shedding for body at rest, D is a characteristic structure dimension perpendicular to the direction of flow, and V is the flow velocity.

The Strouhal number is a function of body shape. Also the Strouhal number may vary with the Reynolds number (Re). Blevins (1977) found a relationship between Strouhal number and Reynolds number for a circular cylinder as shown in Figure 2. As shown in the figure, $S_t \approx 0.2$ for $500 \leq Re \leq 10^5$ (subcritical range). In the range of $Re = 10^5 \sim 10^6$ (transcritical range), there is an upper branch and a lower branch. The upper branch of the curve is for the cylinder with a smooth surface, and the lower branch is for the cylinder with a rough surface.

It is noted that the vortex shedding frequency in the equation of Strouhal number is for a structure without movement. In other words, for a fixed rigid body, vortex shedding is easily be described. However, vibrations of flexible structures induced by transverse wind or ocean current forces are observed in numerous occasions. Therefore, a totally flexible body or a rigid body with flexible support should be considered. Vibrations of a body due to vortices lead to a continuous change in the boundary conditions of the flow and vortices, which may generate a more complex problem due to the interaction between dynamic flow and vibrated structure.

Vortex induced vibration (VIV) is a body-wake nonlinear interaction. Historically, two main experimental methods, free vibration and forced vibration are developed to give insight into the phenomena. The freely vibrating cylinder is much of interest to structural engineers and ocean engineers. Feng (1968) developed several tests for freely vibrating cylinder in wind tunnel. The cylinder is spring-mounted on the wall of the test section. However, such experiments are difficult to interpret, as changes in the reduced velocity (which is shedding frequency normalized by natural frequency) also changes the amplitude ratio (amplitude normalized by diameter of cylinder). Thus, this generates a difficulty for determining the relative importance of the effects on the vibration response. In order to avoid such problems and examine one parameter at a time, forced vibration methods have been employed. The forced vibration experimental method may keep one variable as constant to observe the effect of another. Typically,the forced vibration cylinder is driven at a fixed frequency by using a external mechanism.

Additionally, it is important to note that there is no clear or unique definition of a bluff body. In fact, Sarpkaya (2004) states that the self-regulating “bluff body” does

not exist. It may be described only in general terms and relies on the imagination of readers. In the field of VIV, it is an elastic or elastically mounted body of proper mass, material damping, and shape whose cross-section facing the ambient flow at sufficient Reynolds number gives rise to separated flow and hence to two shear layers, which interact with each other and an unsteady wake.

Investigations on VIV problems are based on experimental, theoretical, and a combined theoretical-experimental analysis. From these investigations, the nature of the motion caused by the flow primarily depends on geometry, mechanical damping, material damping, flow density, flow viscosity, vortex periodicity and structural frequency. Generally, the behaviors observed is the interaction between the fluid dynamic forces and structural dynamic forces of the structure. Based on previous research, the critical features of VIV phenomena may be characterized as

- A shedding natural wake that interacts with the structural motion-induced wake in the near-wake range,
- A structural instability based on unsteadiness in the fluid flow,
- A wake that is controlled by structural motion,
- A possible synchronization (also referred to as "lock-in") phenomenon during the interaction of the flow and structure, and,
- System damping and mass might affect the amplitude of vibration and regarded as an "instability induced by instability".

Some detailed characteristics of the above behavior may be found in references such as Blevins (1977), Bearman (1984), Simiu and Scanlan (1986), Reonard and Roshko

(2001), Blackburn et al (2001), Sarpkaya (2004) and Williamson (2004).

B. Experimental Observations

Experimental evidence indicates that vortex induced vibration (VIV) is a self-excited oscillation of a structure with the driving force originating in the fluid due to vortex shedding at a frequency. The "lock-in" phenomena, which is similar to resonance and related to a synchronization between fluid and structure, is observed in experiments.

Previous test observations focused on the aspects of negative-damping effects, energy source transfers, bandwidth-limited instabilities, effects of mass damping, and "lock-in" conditions. Many experiments, for example, Feng (1968) and Blevins et al (2009), were investigated that lead to a summary as

- Response in water is different from that in air,
- Forced VIV experiments are different from that of free vibration,
- Responses have a jump phenomena and may have hysteresis as shown in Figure 3,
- There are three basic influence factors of VIV phenomena: mass ratio, damping and stiffness of structure.
- Variation of mass ratio affects the response even if the mass-damping ratio is constant,
- The "lock-in" response is larger at low mass ratio.

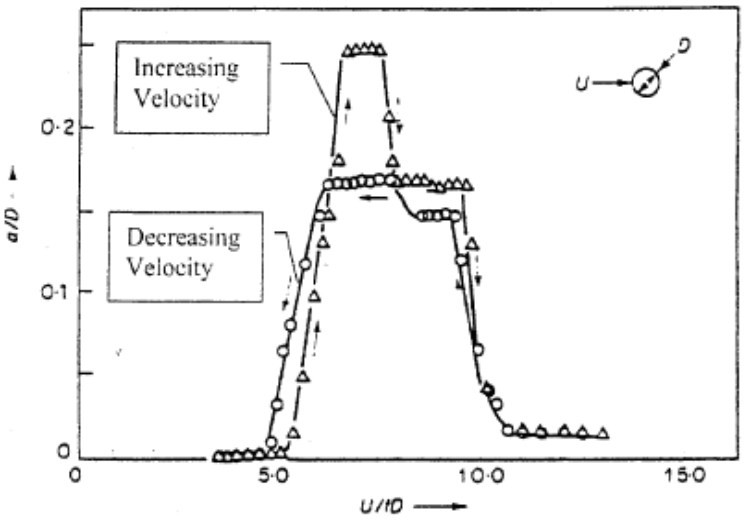

Fig. 3. Jump and Hysteresis Effect (Gowda et al. 1987)

1. Characteristics of Vortex Shedding

When a stationary rigid cylinder with fixed end is placed in a flow, it may lead to a separation in the flow. At low Reynolds number, the flow around the cylinder remains steady until it reaches a certain critical Reynolds number. At the critical Reynolds number, nonlinear interaction between the separated shear layers is developed. These interactions generate the organized and periodic motion vortices. The change of flow passing the cylinder with respect to Re is shown in Figure 4.

When the bluff body (or cylinder) is free to vibrate, certain wake patterns may be induced by body motion, such as the 2S mode (two single vortices per cycle) and 2P mode (comprising two vortex pairs formed in each cycle). Interestingly, if a forced vibration mechanism is introduced, another vortex mode called P+S mode (one single and one pair vortex in a cycle) may be found. The 2S, 2P and S+P modes are the principal modes near the "lock-in" region as shown in Figure 5. The 2P and P+S

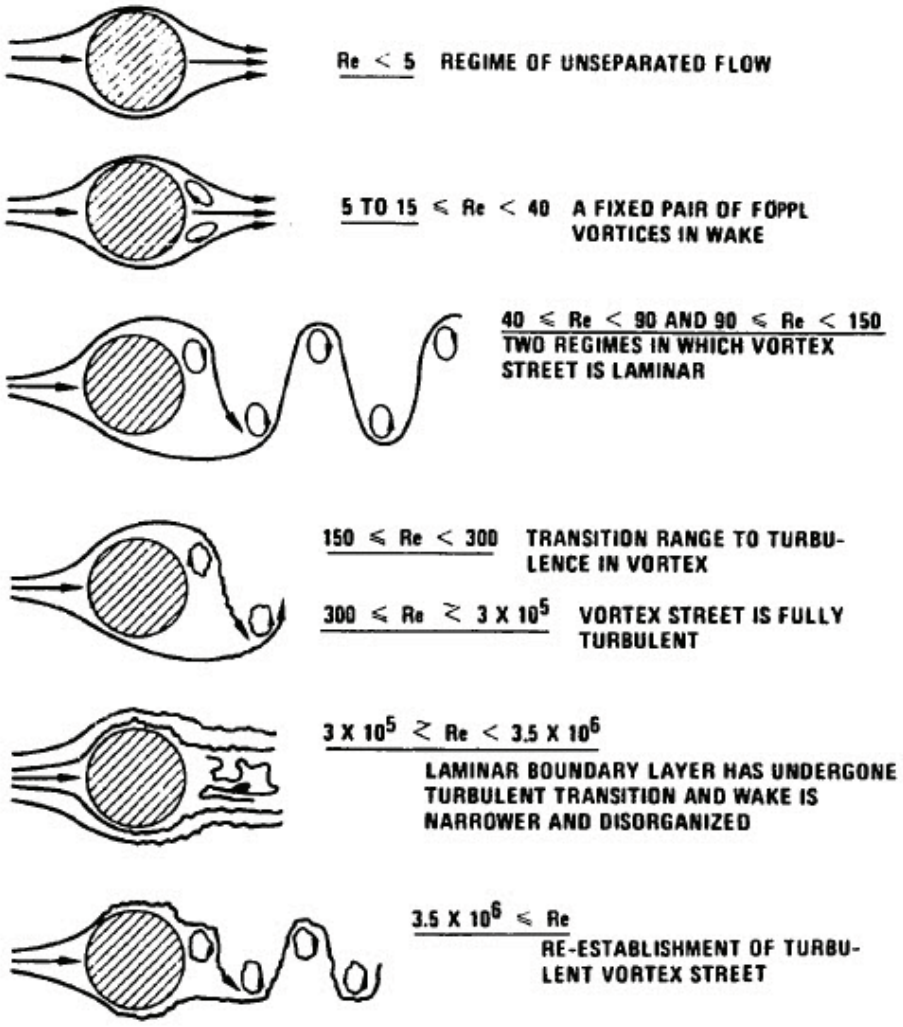

Fig. 4. Vortex Regimes from a Fixed Circular Cylinder (Blevins 1984)

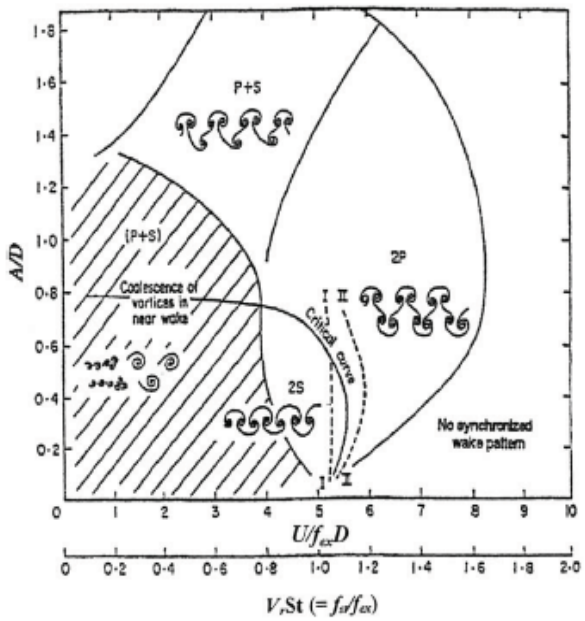

Fig. 5. Map of Vortex Patterns (Williamson and Roshko 1988)

modes have been found in controlled vibration studies in-line with the flow (Griffin 1976). The significance of these modes is that they provide a map of regimes with which certain branches of free vibration may be observed.

2. Free Vibration and Self-excited Motion

The free vibration case is of great interest to structural engineers and ocean engineers, especially for vibration of cables in cable-stayed bridges and mooring systems, as it may represent a significant physical problem with which they are concerned.

Generally, the free vibration tests are conducted in a wind or water tunnel without any external driving mechanism. The structural body is supported by springs or other elastically support systems. Since free vibration is more representative to

the true nature of VIV, the purpose in these studies is to understand the response characters which is derived from time-history response. Feng's (1968) experiments of the cylinder (and also D sections) in the wind tunnel are classical test examples for freely vibrating structures. *Amandolèse* (2010) conducted similar tests for a square cylinder in wind tunnel. Some of Feng's experimental response characteristics have sufficient detail to be used to calibrate models from experiments. The free vibrations indicate VIV is a self-excited vibration. Numerous contributions have been made toward the understanding of the kinematics and dynamics of self-excited vibrations of mostly cylinders.

The statement that VIV is a self-excited oscillation is commonly accepted from free vibration experiments. Umemura et al. (1971) observed from experiment that the aerodynamic damping factor for a cylinder in free vibration acts as a negative damping force for a Strouhal number of 0.2. They also found that the vibrating characters of a cylinder appeared only when the damping force is negative. There is also an additional condition for self-excited motion to be generated, which is observed in the experiments that vibration is possible only when the body mechanical damping is less than the negative damping created by the interaction between the wake and vibrating body.

However, Sarpkaya (1979, 2004) has expressed a view to the contrary: "Apparently the often-used definition of 'self excited ocsillation' is a misnomer". "A vortex-excited oscillation is actually a forced one having a self-excited character also to some degree due to lift force amplification through nonlinear interactions." Cincotta et al. (1966) found that the transverse component of the lift-force acted as a positive damping outside the lock-in region, so that there was negligible body oscillation. In

the “lock-in” range, however, it was observed that there was a great increase in the aerodynamic force, which was “negative damping”.

Sarpkaya (1979) defines a self-excitation as one in which (Den Hartog 1956) “the alternating force that sustains the motion is created or controlled by the motion itself; when the motion stops, the alternating force disappears.” But this definition is proved to be contradicted by rigid body oscillation. For the fixed rigid body, although there is no body motion, the alternating lift force is still present. Another way of looking at the matter is by defining a self-excited vibration as free vibration with negative damping that encompasses the intrinsic character of the process in an appropriate way. The important character of self-excitation as noted by Scanlan and Rosenbaum (1968) is that forces are “of such nature as to feed energy to the system,” which may be “interpreted physically as negative damping terms”. Along with the creation of negative damping, transfer of energy should be considered. For a positive damping in a system, the damping force does negative work. In the case of negative damping, the damping force does positive work on the system, which requires a transfer of energy. Protos et al. (1968) found that the energy transfers from fluid to the cylinder which causes the self-excited vibration.

3. Forced Vibration

Free vibration experiments, for example, Feng’s tests, are difficult to interpret due to the relationship between the reduced velocity (shedding frequency normalized by natural frequency) and the amplitude ratio (Amplitude normalized by Diameter of the cylinder). In order to avoid such issue, forced vibration experiments are employed to consider one factor at a time. This method maintains a constant test condition to

examine the effect of the other. A typical forced vibration experiment of a cylinder is the cylinder driven by an external mechanism at a fixed frequency at a desired amplitude A/D and Reynolds number throughout the range of reduced velocity.

Forced vibration experiments may provide certain insight that may not be obtained from free vibration tests directly. For example, one may examine how a body motion influences its own wake to cause synchronization and other related effects. Also one may examine the formation of the periodic flow. Forced vibration may regularize and idealize almost every aspect of VIV, leading to pure sinusoidal oscillations, forces and almost repeatable wake states.

Through forced vibration tests, Bishop and Hassan (1964) investigated the lift and drag force on a cylinder oscillating in the water, which leads to the conclusion that wake behaves as a nonlinear oscillator initiated a whole line of theoretical models. Sarpkaya (1978) carried out systematic measurements of forces on a rigid cylinder vibrating sinusoidally transverse to a uniform water flow and presented the inertia or added-mass coefficient for various values of A/D in the range of $6 \times 10^3 < Re < 3.5 \times 10^4$. The data obtained from experiment is used in a linear equation of motion to predict the amplitudes of oscillation of an elastically mounted self-excited cylinder. Carberry et al. (2001) subjected circular cylinders to controlled sinusoidal oscillations transverse to a uniform flow at $Re < 10^4$. It is observed that many well-known characteristics of the forces and transitions as the frequency of oscillation passes through the Strouhal frequency. Carberry called them "transition" between the "low-frequency and high frequency state" although the frequency changes only slightly during the "transition".

After Bishop and Hassan (1964), experiments using forced vibrations were conducted by Sarpkaya (1979), Moe and Wu (1990), Sarpkaya (1995), and Carberry et al. (2001, 2005). Some critical issues obtained from forced vibrations are summarized as

- In the synchronization ("lock-in") region, there is a large variation in amplitude and phase,
- Vortex shedding may "lock-in" with structural body not only at $\frac{f_{st}}{f_{ex}} = 1$, but also within a ratio range from 0.5 to 0.9 depending on the normalized amplitude A/D , where D is the diameter of cylinder,
- "Lock-in" occurs if the tuning and the amplitude ratio A/D reach certain critical values,
- Variation of mass ratio affects the response even if the mass-damping ratio is constant,
- There is a nonlinear dependence of the lift-force on the cylinder vibrating amplitude.
- Relatively large random effects exist in the lift force of the cylinder.

4. Influencing Parameters

Parameters that may influence vibration response are investigated and suberized in many documents such as Shiels et al. (2001), Sarpkaya (2004) and Williamson et al. (2004). Sarpkaya (2004) suggests that from a simple dimensional analysis, one may obtain the parameters of "controlling" the transverse vortex-induced vibration of a cylinder. The parameters are density of fluid, dynamic viscosity, velocity of the

ambient flow, diameter of the cylinder, length of the cylinder, spring constant, mean roughness height of the cylinder, structural damping factor, mass of body (with no added mass), mean shear(dV/dy) and taper (dD/dy). In these parameters, mass and structural damping is of most concern by engineers.

The influence of mass is qualified by a parameter called mass ratio (m^*). Mass ratio may be defined as mass of structure divided by displaced mass. Sarpkaya (2004) simplified the mass ratio by $m^* = \rho_m/\rho_f$. Here, ρ_m is the density of structure, ρ_f is the density of fluid. The damping effect is represented by the classical damping ratio (ζ). However, one may find a term referred to as mass-damping ratio ($m^*\zeta$). In fact, Sarpkaya (1979) suggested that the two parameters should not be combined to form a new parameter (or to eliminate an independent parameter). Nevertheless, the mass-damping ratio has been used as a common practice. In addition, Govardhan and Williamson (2002) provide a concept of critical mass. They believe the critical mass would control the behavior of response.

Unfortunately, there is no report to show the determination of damping factor by systematic experiments in vacuum. During the past several decades, damping has been used at various times to represent "damping in vacuum", "damping in still air", "damping in still water", and damping in "flowing test fluid". Griffin et al. (1976) conducted limited experiments to determine the "structural to still-fluid damping" of an elastically supported cylinder. Griffin concluded that the delay of the system in still air was predominantly due to fluid resistance, and the common assumption of negligible "in-air fluid loading" was not valid. The influence of damping on mass is still developing and there is no complete conclusion on the influence of these parameters.

5. "Lock-in" Phenomena

"Lock-in", also known as synchronization, is found for numerous VIV cases. For an elastically mounted structure, it is possible for the wake to synchronize with the motion of the structure.

Large vibration amplitude of related VIV is associated with the "lock-in" effect. Therefore, to some extent, "lock-in" may be considered as an identification of a flow-induced vibration. General structural response without "lock-in" effect is also observed in experiments (Gharib 1999). The maximum amplitude of such response may have a higher magnitude than the corresponding "lock-in" vibrating amplitude under certain circumstances. Thus, for the response to be "lock-in" condition, the time history response must be associated with corresponding frequency curves. And it should be noted that larger amplitude response is not the only criterion for observation of "lock-in".

Some define "lock-in" as $\frac{f_{ex}}{f_{vs}} \approx 1$. However, more recent experiments show even if f_{ex} and f_{vs} are not closed to each other, there may be still large vibration amplitude being observed for a range of damping and mass conditions. This traditional definition has been modified with the development of recent theories and tests. Leonard and Roshko (2001) define the "lock-in" as follows at zero damping and sinusoidal motion. "Lock-in" occurs at only one condition, where "effective" elasticity equals zero. Here, the term "effective" elasticity represents net effect of stiffness and mass effects, as follows

$$k^*_{eff} = k^* - m^*\omega \tag{2.2}$$

where $*$ indicates nondimensional forms, $k^* = \frac{k}{1/2\rho V^2}$, $m^* = \frac{m}{1/2\rho D^2}$, $\omega^* = \frac{\omega D}{V}$. Note: k^* and m^* depend on dynamic pressure.

(Dahl 2008) states that a natural instability of the flow occurs at the Strouhal frequency. When the structure (body) moves, the frequency of vortex shedding may couple with the frequency of structural oscillation. The frequency band increases with increasing amplitude of motion. This property is referred to as wake capture. The ability of a wake to capture the oscillation frequency of the structure results in substantial change of the added mass effects, which may change the natural frequency to an effective natural frequency. This effective natural frequency depends on flow velocity. "Lock-in" is a dynamic equilibrium identified by frequency coupling and a flow-structure energy balance.

In the "lock-in" regime, it is concluded that when a structure vibrates at its natural frequency (f_{air} for engineering application, f_{vac} for detailed scientific research) and approaches a sustained amplitude, the motion of structural vibration governs the shedding frequency of vortices. The linear relationship that agrees with the definition of Strouhal number between the flow velocity and shedding frequency, is no longer valid in the "lock-in" regime. The structure sustains a vibration frequency until it is disturbed by a significant force at a different frequency. This is a key point that shows the different between VIV "lock-in" and a classical mechanical resonance. Under resonance, the oscillator always vibrates at the excitation frequency which is independent of system features.

"Lock-in" is significantly affected by the mass of the structural body and damping of the system. "Mass ratio", "damping ratio" and "mass-damping ratio" are used

to quantify the influence of mass and damping. The stiffness of the structure is also found to be an influencing factor. The term "mass ratio" is defined as body mass divided by displaced mass which quantifies the influence of flow around the body. "Mass-damping ratio" is a grouped term of mass and damping defined as $m^*\zeta$. The non-dimensional damping ratio(ζ) is a characteristic of the structure system. From Lee and Allen (2010), it is observed that lighter or softer stiffness structures have a broader "lock-in" band than a heavier or stiffer structure. Thus, there are three fundamental parameters, mass, damping and stiffness of interest. Which parameter controls the amplitude of response depends upon the ratio of the excitation frequency to the natural frequency. If the ratio is less than one, stiffness governs. For the ratio greater than one, mass is the governing factor. When the ratio approaches resonance conditions (ratio equals to one), damping controls the amplitude.

Parkinson (1989) found two distinct modes of shedding in the "lock-in" regime for a spring-mounted cylinder with a high mass-damping ratio. The different modes of shedding are described as the initial branch of shedding and the lower branch of shedding. Studies by Goverdhan (2000) for the low mass-damping cylinder indicate that a third distinct upper branch existed in addition to the initial branch and lower branch within the regime of "lock in". For low mass damping, both upper modes and lower modes were clearly observed in non-dimensional numerical simulation. Goverdhan et al. (2001, 2005) found experimentally that the value of the normalized frequency is inversely proportional to the mass ratio of the cylinder.

A critical review was conducted by Sarpkaya (2004), in which a comparison of response under different damping ratios was made, as shown in Figure 6. Figure 6 shows the comparison of Feng's data in air, with those obtained by Khalak and

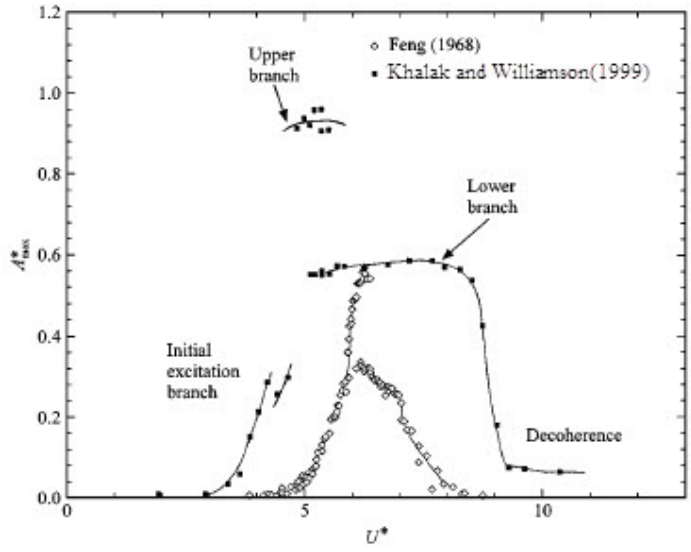

Fig. 6. A Comparison of Data Obtained in Air and Water (Khalak et al. 1999)

Williamson (1999) in water. Feng's data at a higher *Re* has only two branches (Initial and Lower). The Khalak and Williamson data have three branches (Initial, Lower and Upper), a large peak amplitude, and a broader "lock-in" range. Decoherence in Khalak and Williamson data means it is not in the "lock-in" range.

Recent research by Dahl (2008) described the "lock-in" as a dynamic equilibrium of flow-structure interaction. The formation of the vortices is caused by the instability of flow wake located behind the bluff body. If the vortices are triggered by flow perturbations, vortex shedding and excitation of structure is unavoidable. The vortex-induced forces may lead to a change in effective added mass and bring the effective natural frequency close to the wake frequency. Finally, the frequency of vortex shedding may exactly match the effective natural frequency of the structure. As a results, "lock-in" occurs.

C. Mathematical Model of VIV

In order to simulate the phenomena of VIV, the fluid-structure interaction mechanism has been explored with mathematical models to explain the physical phenomena. Based on the fundamental objective of matching body characteristic, engineers have investigated many mathematical models of cylinders for VIV which may be classified as single degree of freedom (SDOF) models, coupled wake-body models and the Birkhoff oscillator model. Some detailed models may be found in Billah (1989), Botelho (1983) and Facchinetti et al. (2004).

1. SDOF Model

The single-degree-of-freedom (SDOF) model for VIV has the advantage of simplicity. SDOF models may be valuable if fluid dynamic characteristics may be taken into consideration in terms of a structural response parameter. The SDOF models may be classified under two divisions: 1) models based on negative damping and 2) models based on forced-coefficient data.

For a fixed cylinder perpendicular to flow the SDOF model may be represented as

$$m\frac{d^2x}{dt^2} + c\frac{dx}{dt} + k = 1/2\rho V^2 D C_L \sin(\omega_s t) \tag{2.3}$$

where, m, c, k represent for mass, damping, and stiffness, respectively. And V, D, C_L represent flow velocity, across-flow dimension, and lift coefficient, respectively. ω_s is the Strouhal frequency given by $\omega_s = \frac{S_t U}{D} 2\pi$.

When the cylinder is free to vibrate, this equation is not appropriate since the

forcing function (right side) is affected by the body motion. In fact, VIV is an interaction between fluid and structure. Simiu and Scanlan (1986) suggested a form of equation for the model based on the negative damping concept, as follows

$$m\frac{d^2x}{dt^2} + c\frac{dx}{dt} + k = F(\frac{d^2x}{dt^2}, \frac{dx}{dt}, x, t) \tag{2.4}$$

Scanlan developed both linear and nonlinear SDOF models. The linear SDOF model is often sufficient in wind and ocean engineering practice. It incorporates aero-damping and aero-stiffness effects with the linear oscillator. The form of this model is

$$m\frac{d^2x}{dt^2} + 2\varsigma\omega_n\frac{dx}{dt} + \omega_n^2 x = 1/2\rho V^2 D[a(K)\frac{dx}{dtD} + b(K)\frac{x}{D} + 1/2C_L(K)\sin(\omega_s t + \phi)] \tag{2.5}$$

where $K = \omega_n D/V$ is the reduced velocity, a, b and C_L are a function of K which must be defined.

However, the model assumes the details of the entire phenomenon are not of concern. Simiu and Scanlan extended the linear model by introducing nonlinear terms starting with a form of the van der Pol equation for the response, and adds a nonhomogeneous forcing term as follows

$$m\frac{d^2x}{dt^2} + 2\varsigma\omega_n\frac{dx}{dt} + \omega_n^2 x = 1/2\rho V^2 D[a(K)(1 - \varepsilon\frac{x^2}{D^2})\frac{dx}{dtD} + b(K)\frac{x}{D} + 1/2C_L(K)\sin(\omega_s t + \phi)] \tag{2.6}$$

where ε is a constant which may represent damping effect from fluid.

Vickery and Basu (1983) developed their model with the essential feature being the representation of forces. The Vickery-Basu model assumed motion-dependent nonlinear damping and a narrow-band random force induced by vortex-shedding.

The models discussed above are models based on the negative damping conception. Force-coefficient data based models are required next. The fundamental requirement of such models is the use of force-coefficient data from experiments.

Sarpkaya (1978) and investigated force-coefficient models. Sarpkaya obtained a set of experimental data by measuring the forces on a rigid cylinder which was forced to vibrate harmonically transverse to the uniform flow. In his method, the transverse force acting on the body was expressed as

$$\ddot{x} + 2\zeta\dot{x} + x = a\Omega^2(C_{mh}\sin\Omega t - C_{dh}\cos\Omega t) \tag{2.7}$$

where a is constant and Ω is the ratio of excitation frequency to natural frequency of the system.

Staubli conducted the analogous experiments by assuming a different form of the lift-coefficient for the model. Staubli's method assumes lift-coefficient in the form as

$$C_L(t) = C_{L0}(t)\cos(\omega t + \phi) + C_{LK}(t)\cos(\omega_K t) \tag{2.8}$$

where C_{L0} is associated with oscillation at the same frequency as cylinder motion; C_{LK} has its origin in *Kármán* vortices, K stand for von *Kármán* vortices, ϕ is the phase shift between displacement, and C_L is the lift coefficient.

SDOF models are simplified and may be valuable for engineering response calculations. However, SDOF models may not decsribe the nature of VIV. Thus, more accurate mathematical models were developed.

2. Coupled Wake-body Models

Compared with the SDOF model, the significant difference of coupled models is that the coupled model introduced the form of equations which are associated with fluid dynamics. The fundamental motivations of the coupled model are to obtain a better match of theory with the observed structural response and to predict the wake characteristics and structural behavior that are observed in the experiment. In the coupled models, the wake from the vortices is treated as a separate oscillator. Therefore, this model is often termed as the wake oscillator models. There are many coupled models based on different assumptions of the wake oscillator.

Hartlen and Currie (1970) simulated the fluid dynamics of VIV by introducing a form of the van der Pol equation coupled to the cylinder motion by a linear dependence on cylinder motion which they called a "soft" fluid oscillator. This model (called the H-C model) emphasized the nonlinear nature of the wake. However, it is noted that the body-wake coupling effect is modeled linearly.

The form of the H-C model is

$$\begin{aligned} \ddot{x} + 2\zeta\dot{x} + x &= a\Omega^2 C_L \\ \ddot{C_L} - a\Omega\dot{C_L} + \tfrac{\gamma}{\Omega}\dot{C_L}^3 + \Omega^2 C_L &= b\dot{x} \end{aligned} \tag{2.9}$$

where C_L is lift coefficient, a, b, γ are constant, and $\Omega = \frac{f_{vs}}{f_{vac}}$.

Skop and Griffin (1973) extended the approach to the real engineering system by assuming the lift-coefficient satisfies a modified Van der Pol equation. In later papers, the lift equation in the model was included more additional terms to create

a small shift in the predicted response frequencies. The lift equation was of the form

$$\ddot{C_L} - \omega_s^2 C_L - (C_{L0}^2 - C_L^2 - \frac{\dot{C_L}}{\omega_s})(\omega_s G\dot{C_L} - \omega^2 H C_L) = \omega_s F \frac{\dot{x}}{D} \tag{2.10}$$

where C_{L0} is the lift coefficient of a statinary cylinder and F, G, H are parameters.

Based on the consideration of fluid mechanics, Dowell (1981) presented a phenomenological coupled model. The equation of motion for structure is

$$m(\ddot{x} + 2_n\dot{x} + {}_n^2 x) = \frac{1}{2}U^2 D C_L \tag{2.11}$$

The equation of motion appears similar to the SDOF model. However, for the equation for C_L, Dowell introduced the fluid mechanical requirement on fluid-oscillator. Based on the consideration for low frequency, high frequency and small lift-coefficient condition, the coupled lift-coefficient equation could be obtained as

$$\ddot{C_L} - \varepsilon(1 - 4\frac{C_L}{C_{L0}})\omega_s^2 \dot{C_L} + \omega_s^2 C_L = -B_1 \frac{D}{V^2} x + \omega_s^2 [A_1(\frac{\dot{x}}{U}) - A_3(\frac{\dot{x}}{U})^3 + A_5(\frac{\dot{x}}{U})^5 - A_7(\frac{\dot{x}}{U})^7] \tag{2.12}$$

where A_i, B are constants. The model has improved their ability to match experimental results.

3. Model Based on the Birkhoff Oscillator Concept

This model was proposed for the determination of the Strouhal number of a stationary cylinder, and Marris (1964) extended it to a vibrating cylinder by considering the body-wake system to act as an airfoil. This model uses a so-called Birkhoff oscillator which is a fixed length, angularly oscillating lamina, for the so called “dead-air” region

behind a stationary cylinder. A general form of this model is

$$\begin{aligned} I\ddot{\theta} + c_w\dot{\theta} + k_w(\theta - \theta_0) &= T \\ m\ddot{x} + c\dot{x} + kx &= F \end{aligned} \tag{2.13}$$

where m, c, $k4$ are body parameters, c_w ,k_w are wake parameters; is the instantaneous wake rotation angle and $_o$ is angle between the flow velocity; I is wake inertia; and, F and T are interaction forces of the wake on the cylinder and driving torque on the wake respectively.

D. Closing Remarks

From the brief review, VIV is a self-excited structural vibration problem. In the experiment, free vibration method and forced vibration method are used to investigate the nature of this problem. “Lock-in” as a distinguished phenomena may be observed in experiments no matter conducted in water or air. It may be considered a basic phenomenon in VIV, but not necessarily a consequence. “Lock-in”, or synchronization, is primarily frequency synchronization. The shedding frequency from a body in motion locks in with the excitation frequency of the body, and shedding vortices and structure vibration approach to a common frequency. When a structural body is in the range of “lock-in”, the vibration frequency of the body may be near the natural frequency of system but not necessarily the same. “Lock-in” may be influenced by mass, damping, and stiffness of structures. The governing parameter of a system may be determine by the ratio of excitation frequency to natural frequency of system. In addition, three fundamental mathematical models are presented. The SDOF model is a simplified model which may not well consider the interaction between structures and flows. The coupled wake-body model might be the “better” model to fit the

experimental observation.

CHAPTER III

EXPERIMENTAL BACKGROUND

A single-degree-of-freedom (SDOF) system is employed to investigate the fundamental phenomena of VIV in pitch oscillation. Measurements are focused on the shedding frequency from the rigid plate (for both body at rest and body in motion), the amplitude of vibration and the vibration frequency. A simple test apparatus called the Linear Rotational Test System (LRTS) was developed as the basic platform for each experiment in the $2' \times 3'$ low-speed wind tunnel in the Aero and Fluid Dynamics Lab at Texas A & M University. An empirical-analytical model is developed to obtain a preliminary view of response.

A. Simple Analytical Mode

A SDOF model for VIV has the advantage of simplicity. SDOF models may be valuable for the engineer if the aerodynamic characteristics is considered in terms of a structural response parameter.

The equation of motion (EOM) for the system under forced vibration is written as

$$I\frac{d^2\theta}{dt^2} + c\frac{d\theta}{dt} + K_\theta\theta = M(t) \tag{3.1}$$

where I is the mass moment of inertia, θ is the pitch angle, K_θ is the pitch spring constant, c is the pitch damping coefficient and $M(t)$ is the excitation moment.

By assuming the system is under a harmonic excitation, the EOM for pitch

motion may be rewritten as

$$\frac{d^2\theta}{dt^2} + 2\zeta\omega_{vac}\frac{d\theta}{dt} + \omega_{vac}^2\theta = \frac{M_o \sin(\omega_{ex}t)}{I} \tag{3.2}$$

where $\omega_{vac} = \frac{K_\theta}{I}$ and $2\zeta\omega_{vac} = \frac{c}{I}$.

Eqn (3.4) consists of two components, the structural characteristics and aerodynamic characteristics. The left side of the equation presents the characteristics of the structure and right side indicates characteristics of the fluid. Considering structure response, the solution θ has a transient response and a steady-state response, and may be assumed as

$$\theta(t) = \theta_T + \theta_{SS} \tag{3.3}$$

where $\theta_T = e^{-\zeta\omega_{vac}t}[A\cos(\omega_{air}t) + B\sin(\omega_{air}t)]$ is the transient response due to system characteristics and $\theta_{SS} = C\cos(\omega_{vac}t) + D\sin(\omega_{vac}t)$ is the steady-state response due to excitation load, A, B, C, D must be determined by initial conditions. The response $\omega_{air} = \omega_{vac}\sqrt{1-\zeta^2}$ is the damped frequency of system in air and ω_{vac} is the true natural frequency of system measured in a vacuum.

Due to the exponential term of the response, the transient component will quickly decay and the total response is dominated by the steady-state response. Thus, if one considers only the steady-state term, substitutes it into the EOM, collects the sin and cos terms to solve C and D, one find,

$$\begin{aligned} C &= \frac{M_o}{K_\theta}\frac{-2\zeta\beta}{(1-\beta^2)^2+(2\zeta\beta)^2} \\ D &= \frac{M_o}{K_\theta}\frac{1-\beta^2}{(1-\beta^2)^2+(2\zeta\beta)^2} \end{aligned} \tag{3.4}$$

where $\beta = \frac{\omega_{ex}}{\omega_{vac}}$ is the ratio of excitation frequency to natural frequency of system.

The θ_{SS} term may be written in phase-lag form as

$$\theta_{SS} = \sqrt{C^2 + D^2}\sin(\omega_{ex}t - \phi) = \Delta_{st}\lambda\sin(\omega_{ex}t - \phi) \tag{3.5}$$

where $\phi = \arctan(\frac{2\zeta\beta}{1-\beta^2})$ is a phase angle, $\frac{M_o}{K_\theta} = \Delta_{st}$ is the static deformation , and $\lambda = \frac{1}{\sqrt{(1-\beta^2)+(2\zeta\beta)^2}}$ is the amplified factor.

The aerodynamic load term M_o is expressed as

$$M_o = qScC_m \tag{3.6}$$

where $q = 1/2\rho V^2$ is the dynamic pressure, S is the area of the plate which is $chord(c) \times span(s)$, C_m is the aerodynamic moment coefficient.

Substituting Eqn (3.8) into Eqn (3.7), the amplitude of response (Θ) is

$$\Theta = \frac{\rho V^2 c^2 s C_m}{2K_\theta}\lambda \tag{3.7}$$

Introducing the Strouhal number and non-dimensional system parameters, the amplitude of response may be written in a dimensionless form as

$$\Theta = \frac{1}{m^*}\frac{1}{S_t^2}\frac{1}{2\pi^3}\frac{C^2}{r_g^2}\beta_{st}C_m\lambda \tag{3.8}$$

where the non-dimensional parameters are defined as
$r_g^2 = I/m$ is the radius of gyration
$m^* = \frac{m}{\frac{\rho\pi c^2 s}{4}}$ is the mass ratio
$S_t = \frac{f_{st}C}{V} = \frac{\omega_{st}c}{2\pi V}$ is the Strouhal number
$\beta_{st} = \frac{\omega_{st}}{\omega_n}$ is the frequency ratio

Eqn (3.10) indicates the amplitude of oscillation is a function of mass ratio and

shape of structure body. For a certain structure, m^*, S_t, c, r_g, β_{st} are constants. The dimensionless equation indicates that the amplitude of response is only a function of the aerodynamic moment coefficient (C_m). The relationship may be written as

$$C_m = \psi\Theta \tag{3.9}$$

where $\psi = \frac{m^* S_t^2 r_g^2 2\pi^3}{\beta_{st} C^2 \lambda}$ has been considered as a coefficient.

Introducing the van der Pol equation, the wake oscillator is defined as

$$\ddot{C_m} + \varepsilon\beta_{st}(C_m^2 - 1)\dot{C_m} + \beta_{st}C_m = A_m\dot{\theta} \tag{3.10}$$

where ε is the air damping ratio and A_m is a reference amplitude.

The SDOF model may be formed as follows

$$C_m = \psi\Theta \tag{3.11a}$$

$$\ddot{C_m} + \varepsilon\beta_{st}(C_m^2 - 1)\dot{C_m} + \beta_{st}C_m = A_m\dot{\theta} \tag{3.11b}$$

It should be noted that the amplitude Θ is also a function of time. Therefore the right hand of Eqn (3.13-b) may be written as $A_m[\dot{\Theta}\sin(\omega t - \phi) + \omega\Theta\cos(\omega t - \phi)]$. Substituting Eqn (3.13-a) into Eqn (3.13-b) yields

$$\psi\ddot{\Theta} - [A_m\sin(\omega_{ex}t) - \varepsilon\beta_{st}(\psi^2\Theta^2 - 1)\psi]\dot{\Theta} + [\psi\beta_{st}^2 - A_m\omega_{ex}\cos(\omega_{ex}t)]\Theta = 0 \tag{3.12}$$

The amplitude of response may be solve by Eqn (3.14). A simple simulation based on the model is developed. The time-history response (shown in Figure 7) has been compared with a known experiment response (shown in Figure 8) based on the same system and test parameters (shown in Table I). Compared with the test results,

Table I. Test Parameters

Parameters	Values
ψ	0.403
ε	0.01
β_{st}	0.95
ω_{st}	53.4 (rad/s)
A_m	0.43 (rad)
θ_0	0.061 (rad)
$\dot{\theta_0}$	46.7 (rad/s)

via introducing the van der Pol oscillator, SDOF model shows certain features of the test results. Although it may not reflect the random fluctuation of oscillation until introducing statistical parameters, it may indicate the amplitude of response one may concern. From Eqn (3.9) and Eqn (3.10), the amplitude is a function of stiffness, mass ratio and radius of gyration. Thus, a lighter and softer structure may have a large response amplitude under a certain excitation force.

B. Design of Apparatus

The Linear Rotational Test System (LRTS) which provides linear rotational motion for the mounted body. In this research, the body is a flat plate constructed of balsa wood. Such a system is illustrated in Figure 9. An isometric view of the entire test setup is shown in Figure 10.

The flat plate is mounted on the support system at both ends of the plate. Motion is constrained to rotation only by a bearing. Thus, the motion is a single

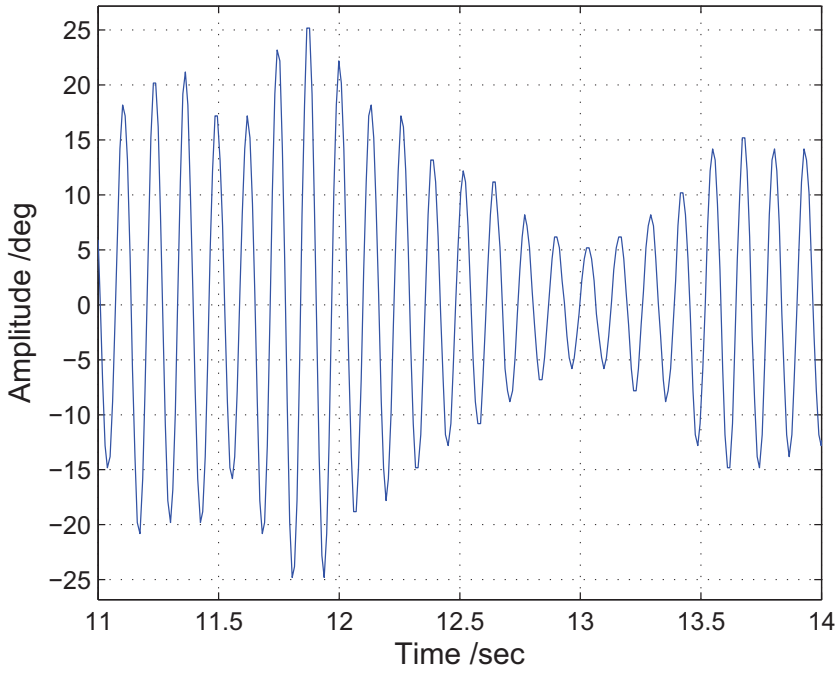

Fig. 7. Time-history Response under "Lock-in"

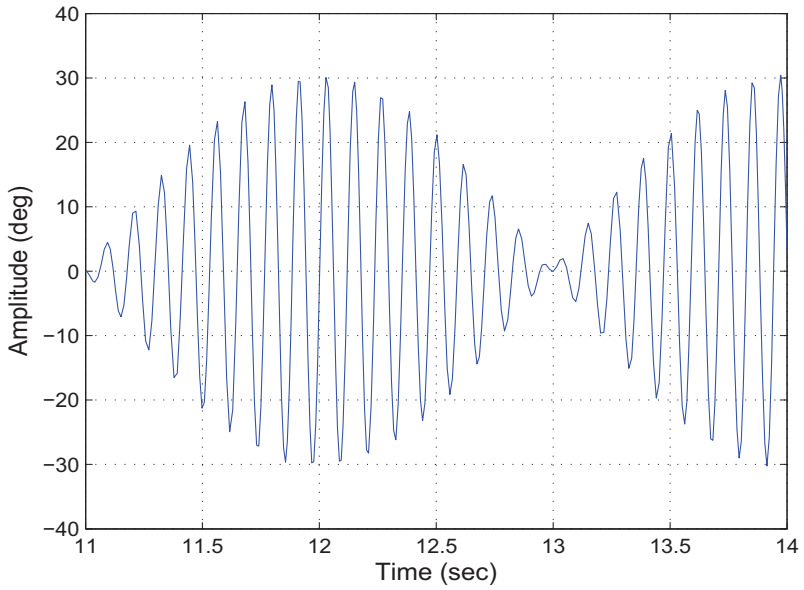

Fig. 8. Predicted Response under "Lock-in"

degree of freedom in rotation. As seen in Figure 10, the plate is mounted vertically in the test section to eliminate the influence of gravity. As shown in Figure 11, there are two separate parts of the moving mechanism: one is fixed to the top of test section (top side) another one is fixed to the bottom side. The top side is composed of the linear spring, bearing, pitch cam and the top shaft. The bottom side is composed of a bearing, the optical encoder and the bottom shaft. The plate is connected to the rotational shafts at each ends via bolts.

The flat plate is built with balsa wood, which is chosen to minimize mass of the system. A view of the plate is shown in Figure 10. This plate has been designed as a "bridge deck" structure as shown in Figure 12. A thick balsa sheet has been selected to the flat plate facing the incoming flow. As support structure, two beams across

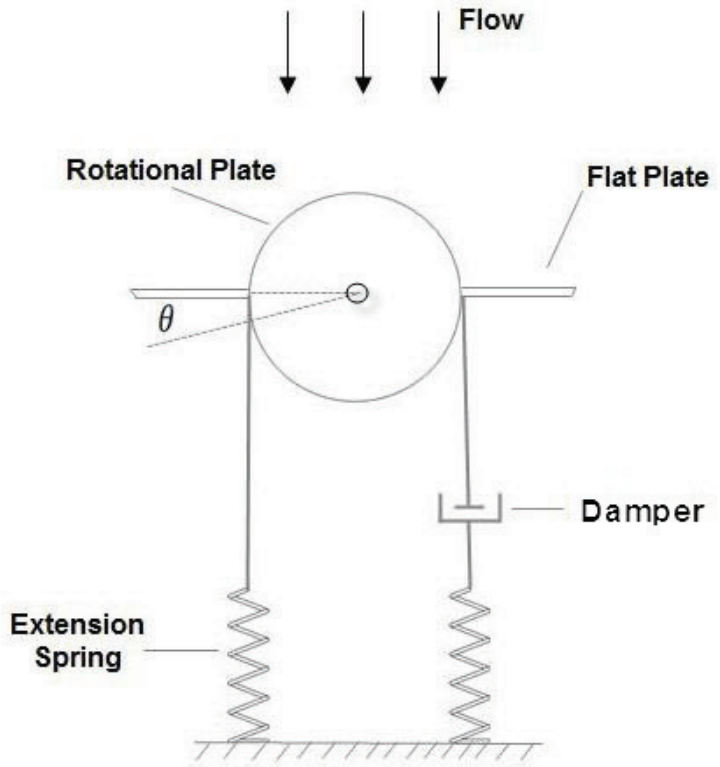

Fig. 9. Schematic View of LRTS (mounted on the topside)

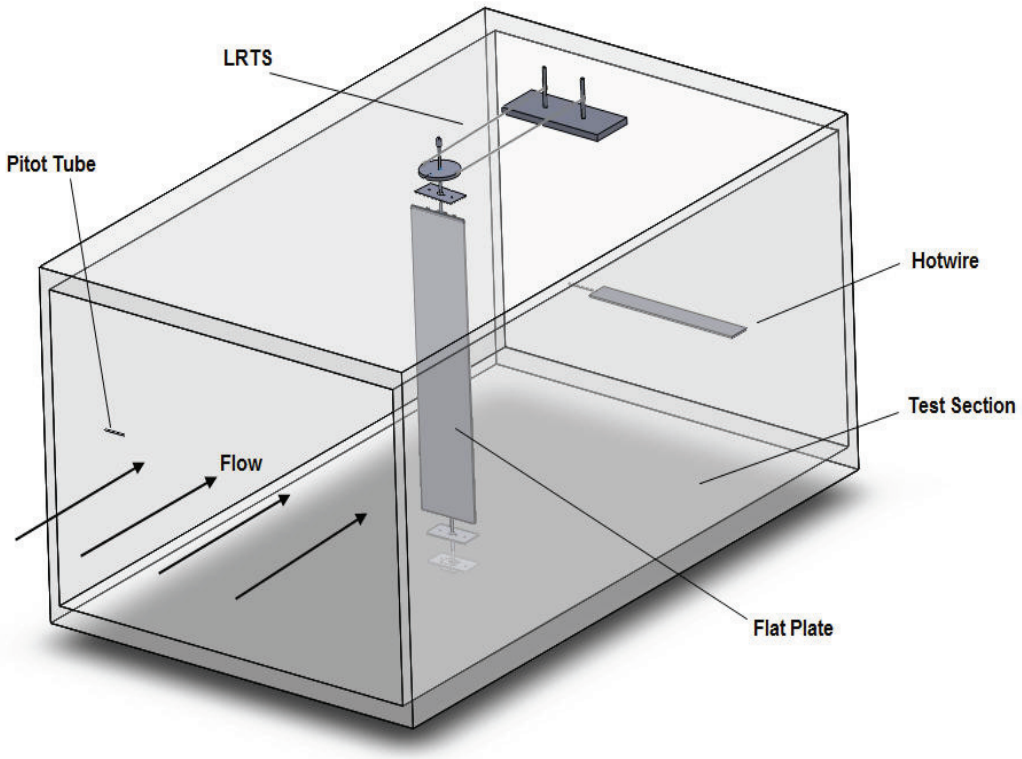

Fig. 10. Isometric View of the Test Setup

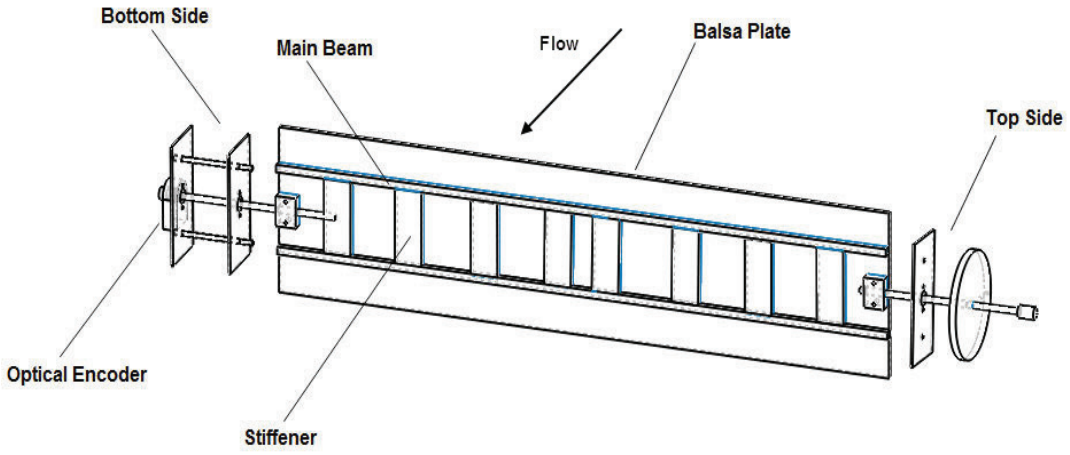

Fig. 11. Plate Structure and Support System

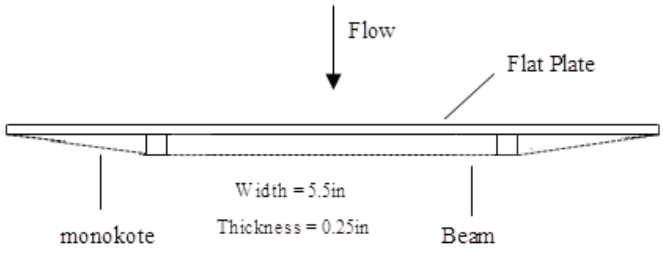

Fig. 12. Cross Section of Plate Structure

the plate are used as the main beam span of the structure. Eight stiffeners have been placed between two beams. In addition, both ends of the plate have been enforced by plywood plate for connecting with moving mechanism. Finally, monokote is used to cover the surface of the structure for maintaining sharp edge and keep the plate surface smooth. Photographs about the experimental equipment are shown in Appendix.

Since the extension springs is linear in the desired test range, and pitch cam is a circular plate, the equivalent rotational spring is linear, as shown

$$K_\theta = 2R^2k \tag{3.13}$$

where k is the stiffness of linear extension spring. R is the radius of pitch cam.

The stiffness of the spring is selected by the "lock-in" frequency condition. From the literature, it is clear that there is a range in which shedding frequency is near the vibration frequency, so that "lock-in" may occur. Based on such assumptions, the procedure of selecting spring constant is listed as follows

- Assume $S_t = 0.145$ (Blevins 1984) for this flat plate, and calculate the Strouhal frequency based on $f_{st} = S_t V/D$,
- Calculate the natural frequency of the structure in vacuum as $f_{vac} = \frac{1}{2\pi}\sqrt{\frac{K_\theta}{I}}$, where I is the entire system's mass moment of inertia,
- Assume $f_{vac} = f_{st}$, and solve for K_θ, then solve for k,
- Choose the spring constant within the range of $\pm 25\%$ of k. The range chosen here may not affect the test results. Larger range may increase the chance to capture "lock-in".

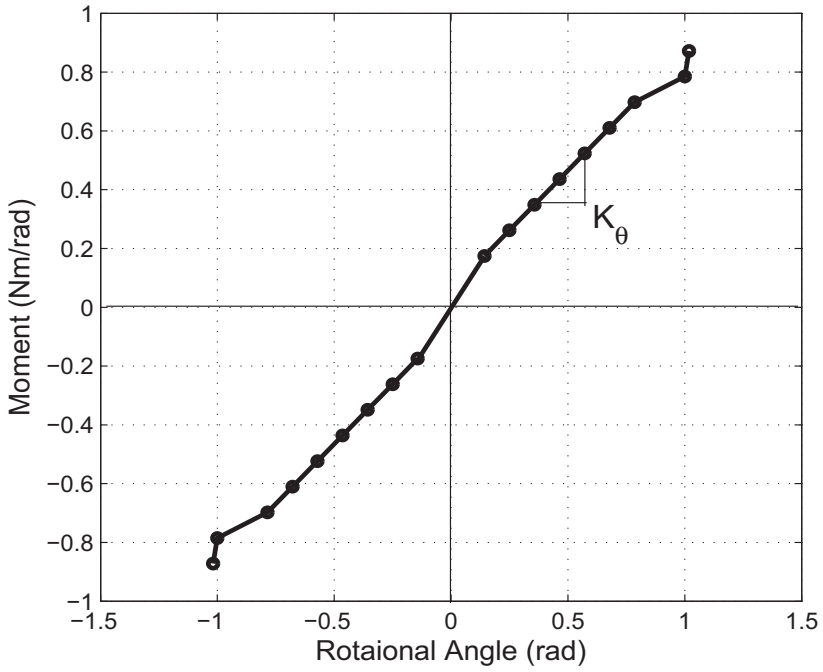

Fig. 13. Moment-rotation Curve

The moment-rotation curve is shown in Figure 13. This curve shows that in the range from $-1.5\ rad$ to $+1.5\ rad$, the spring would be in the linear range of extension.

The Strouhal frequency is measured by hot-wire anemometry and the vibration frequency is measured by using the out put of an optical encoder. The data acquisition system is shown in Figure 15. The physical parameters measured for LRTS, including measured masses, moment of inertia, size of each part, spring constant and damping coefficients are provided in Table II.

Table II. System Properties and Test Parameters

Parameters	Values
Mass of Plate	0.0838(kg)
Total Mass	0.166 (kg)
Inertial	$1.82 \times 10^{-4}(kgm^2)$
Spring Constant	102.8 (N/m)
Rotation Spring Constant	$0.41(Nm/rad)$
Damping Ratio	0.023
Chord of Plate	0.14(m)
Span of Plate	0.597(m)
Radius of Top Plate	0.045(m)
Frequency in Air	7.55 (Hz)
Frequency in Vacuum	7.62 (Hz)

C. Measurement of Vortex Shedding

Shedding frequencies from the structure (at rest and in vibration) have been measured by hot-wire equipment. One hot-wire device is required in the test. The device is horizontally supported on the side of the wind tunnel test section, as shown in Figure 10. The distance between plate and hot-wire is 14 inch (0.36 m). The device may travel through a range of 34 *in* which is approximately the span of the test section. This movable device measures both the shedding frequency and characters of the vortex shedding from the flat plate, simultaneously.

The hot-wire device measures the change of wind velocity directly. Then, the signal is transformed into shedding frequency by Fast Fourier Transformation (FFT) in Labview and Matlab. FFT transfers the time domain signal to frequency domain signal, from which shedding frequency is obtained. The free stream velocity of the test section is determined via a Barocell precision pressure transducer connected to a Pitot probe in the test section. Simultaneously, the velocity is obtained by a digital manometer for verification.

D. Measurement of Structural Vibration

The information obtained from the structure vibration is primarily amplitude, frequency of vibration, and applied moment loads acting on the structure. The information that is directly obtained from tests is the amplitude and frequency of vibration via optical encoder. Loads acting on the structure are be calculated from equations as

$$M_\theta = K_\theta \theta = 2R^2 k\theta \tag{3.14}$$

where k is the extension spring constant, R is the radius of circular plate and θ is rotational angle.

Pitch motion (rotation) is measured with the US Digital E2-1024-375-H3 Optical Encoder. The encoder that provides measurement directly is connected to the end of bottom shaft. Data collected from the encoder is processed in Labview for post-process. After post-process, information such as amplitude and frequency of vibration is determined. Free vibration of the system sample test is conducted via the measurement describe above. Time-history response is shown in Figure 14

E. Data Acquisition

Figure 13 shows the diagram of the data acquisition system.

Measurement of the flow speed is provided by both manometer and Barocell precision pressure transducer. Pressure measured directly from Barocell is converted to velocity. Since data from the manometer is the flow velocity directly, the manometer is used for monitoring flow velocity in real time.

Data from plate vibration is obtained from the digital optical encoder. A data translation D/A panel (National Instrument NI-USB-6009) transfers the signal from the encoder to the computer in which Labview is installed. A Labview code called "THA" (represents Time History Analysis) will show a live time-history record of vibration. Amplitudes and frequencies are obtained by post-process. Hot-wire equipment provides the shedding frequencies of the plate (at rest and in vibration) as

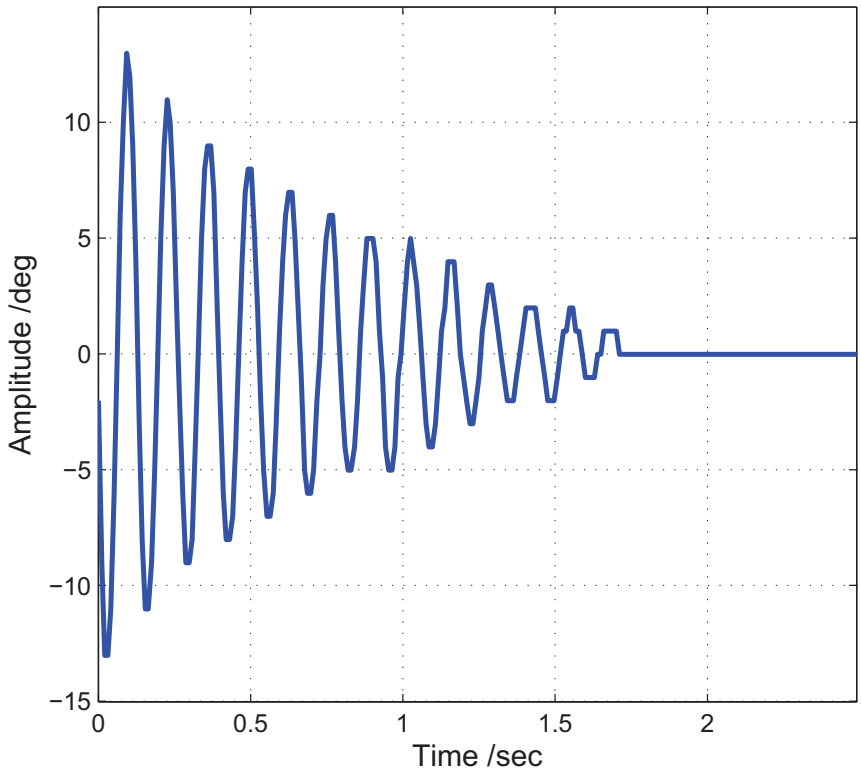

Fig. 14. Free Vibration Response

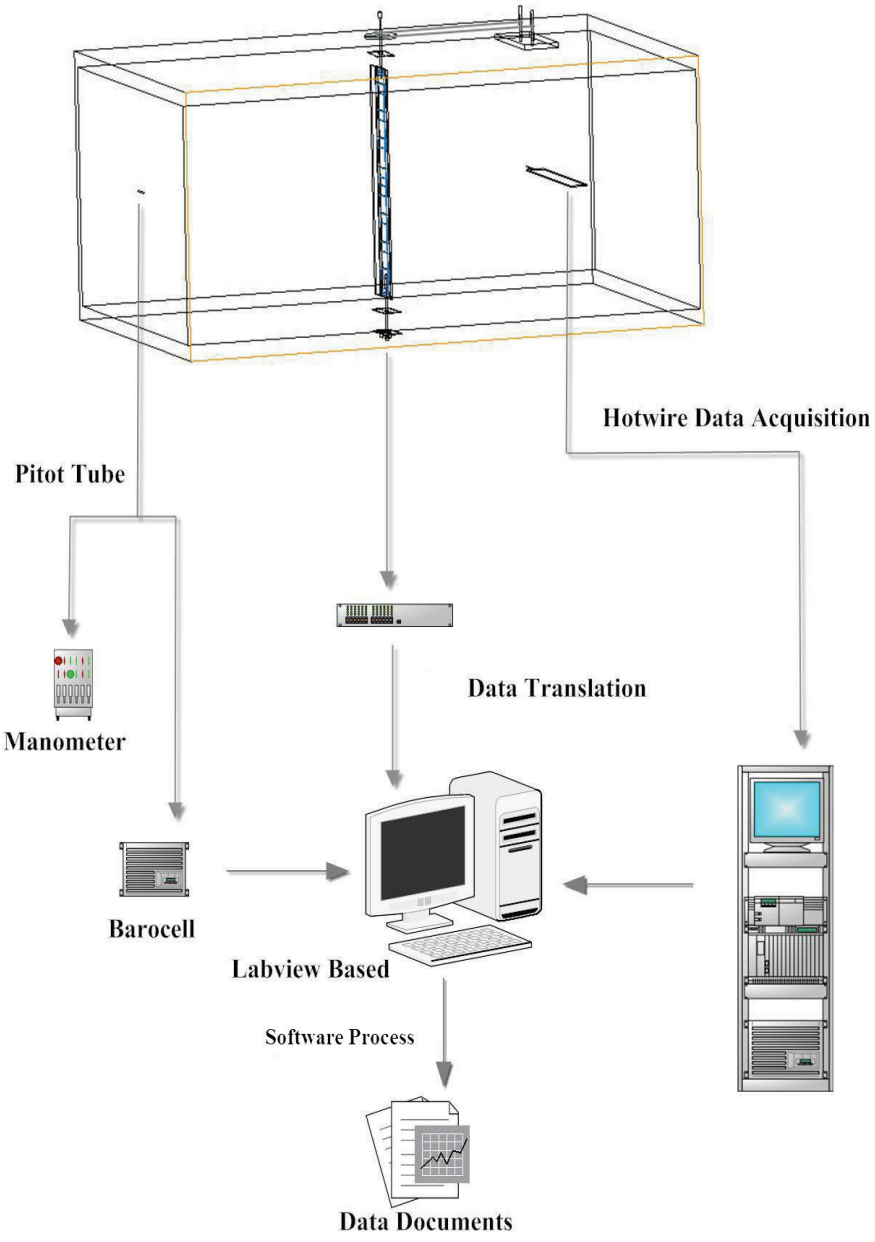

Fig. 15. Diagram of Data Acquisition System

shown in the right side of Figure 15. All data is collected by the computer and sent to post-process. In the post-process, Matlab based codes are used for analysis to provide final data.

CHAPTER IV

EXPERIMENTAL STUDIES

This chapter describes the details of measurement and test results on both stationary and vibration tests. The stationary tests primarily focus on the measurement of Strouhal number of the flat plate and wake character from stationary plate. The vibration tests primarily focus on the measurement of shedding frequencies from vibrating body and the frequencies of structural vibration at different wind velocities. "Lock-in" has been observed in the vibration tests.

A. Measurement of Strouhal Number

A plate fixed at both ends was placed in the wind tunnel. The plate was placed across the flow (90 degree with flow) as shown in Figure 16. Shedding frequencies of vortices generated from the flat plate were measured by the hot-wire anemometry located at the downstream of the flow with a distance of $15in$ $(0.381m)$ from the plate. The change of voltage signal was transferred from the time domain to frequency domain by Fast Fourier Transformation to obtain the shedding frequency (Strouhal frequency) from the stationary plate. As stated in the second chapter, Strouhal number for the plate may be defined as

$$S_t = \frac{f_{st}C}{V} \tag{4.1}$$

where f_{st} is the Strouhal frequency, C is the chord of plate and V is the flow velocity. Based on the equation above, one may obtain the Strouhal number via the Strouhal frequency measured from hot-wire anemometry.

The Strouhal frequencies change with various velocities. For a certain shape,

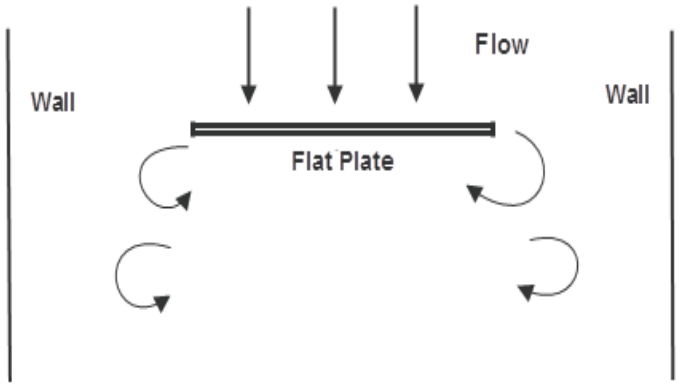

Fig. 16. Plate in Flow

the Strouhal frequency increases with an increasing flow velocity. However, Strouhal frequency may be a constant for a certain shape with a certain orientation with the flow. In the stationary tests, wind velocity is increased from approximately $3m/s$ to $22m/s$ with increments of $1m/s$. Simultaneously, the Reynold's numbers, shedding frequencies and Strouhal numbers are recorded as described in Chapter III. It is well known that Strouhal number is a function of Reynold's number and the geometry of structure. Figure 17 shows the variation of shedding frequency with wind velocity. Figure 18 shows the relationship between Reynold's numbers and Strouhal numbers.

From Figure 17, with increasing of wind velocity, the shedding frequency increases which reflects the linear relationship between f_{st} and V indicates by Eqn (4.1). Theoretically, since C is a constant and S_t is also constant, the shedding frequency is proportional to flow velocity. Figure 18 shows Strouhal number as a constant with the increasing of Reynold's number in this certain range. This plot agrees with Blevins (1977) that vortex shedding persists within the entire subcritical range of the Reynolds number as described in Chapter II. The straight horizontal line

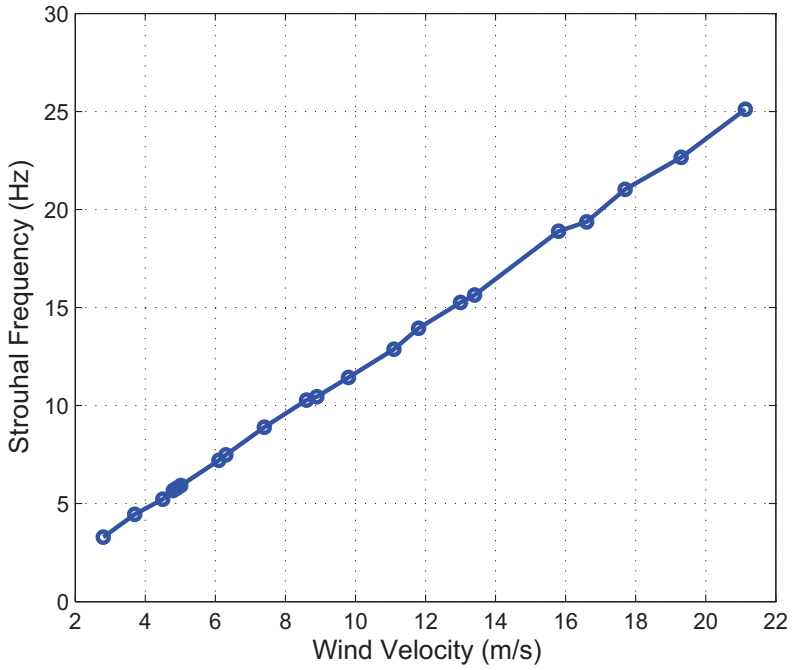

Fig. 17. Wind Velocity versus Shedding Frequency for the Stationary Body

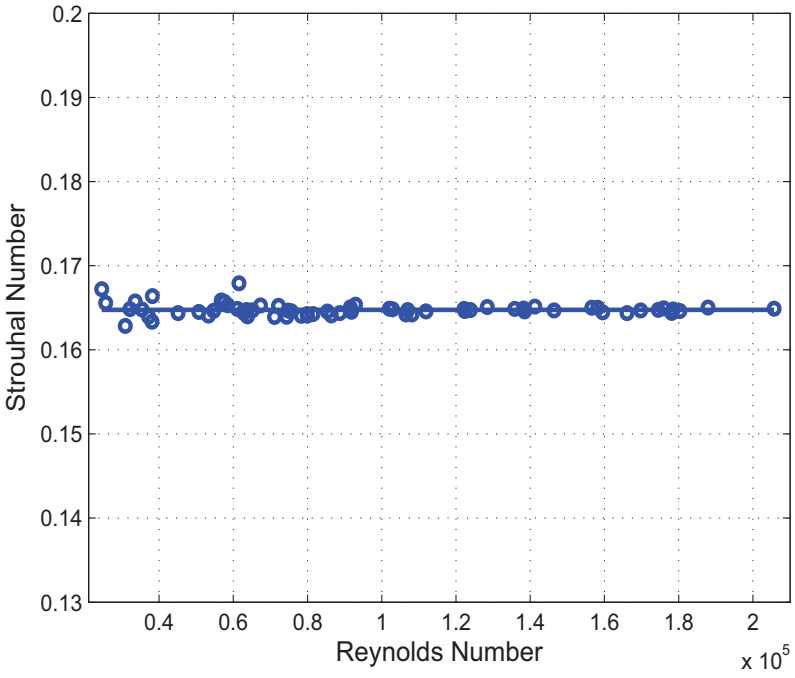

Fig. 18. Strouhal Number versus Reynold's Number

in Figure 16 represents the equivalent Strouhal number in the tests as a whole. The value obtained from fitted curve is $S_t = 0.1647$ for this flat plate.

B. Wake from Stationary Plate

Based on the same setup and equipments as in the measurement of Strouhal number, a set of tests focused on the wake and flow visualization has been conducted. As illustrated in Chapter III, the hot-wire anemometry is moved from one wind tunnel wall to the other wall. This provides the position to measure the shedding frequency and wake strength in for a range. Twenty-one observation points, as shown on the hot-wire measurement line in Figure 19, are selected. The middle point located at the center line of the wind tunnel test section perpendicular to the flat plate. There are sampling twenty points distributed along the measurement line with the spacing of 1 in $(0.0254m)$.

Time domain signals obtained from hot-wire anemometry are transferred to frequency domain signals. Figure 18 shows the frequency domain signals at each observed point at the speed of 9 m/s, as an example. The X-axis of the figure represents the location of observed point. The Y-axis represents shedding frequency, and Z-axis is the normalized amplitude of the spectrum (by Z/Z_{max}). The amplitude is a relative number, which may be used for seeking the relative strength of vortex shedding from the stationary plate.

At 9 m/s, the theoretical Strouhal frequency is $f_{st} = \frac{S_t V}{C} = 10.6$ (Hz). The experimental Strouhal frequency may be obtained from Figure 20, which agrees with

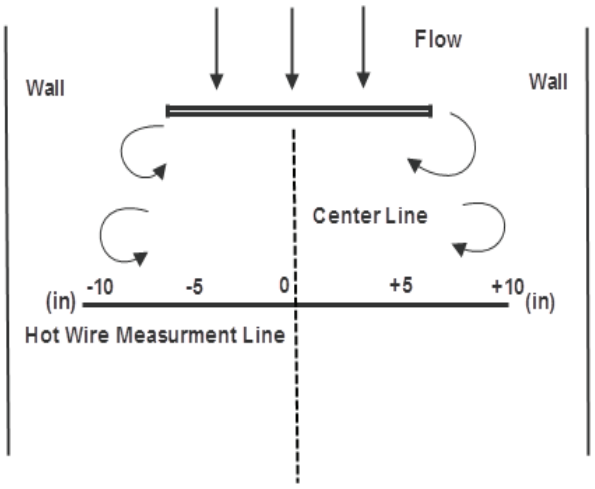

Fig. 19. Measurement of Vortex Shedding

the theoretical value. It is interesting to note that for points near the center line, a second peak at 22.3 (Hz) may be observed in absence of the first peak. It suggests the shedding frequency at those points are doubled due to the overlap of two vortices. For example, at the test point locates 1 inch from the center line, it appears two peaks which reflects a weak overlap of two vortices. From Figure 20, it is obvious that at the point located ± 5 *inch* from center line, the strength of vortices goes to the maximum. Figure 21 shows three typical amplitude power spectrums of vortex shedding (log scale) at different point of observation.

The test results shown in Figure 21 is obtained from a stationary test at $V = 7.0\ m/s$, as an example. Figure 21(a) is the most common spectrum which is referred to as a single peak spectrum with only first peak. Figure 21(b) is referred to as a double peak spectrum with first peak in governing. Figure 21(c) is considered as a single peak spectrum with only the second peak. Further experiments indicate that

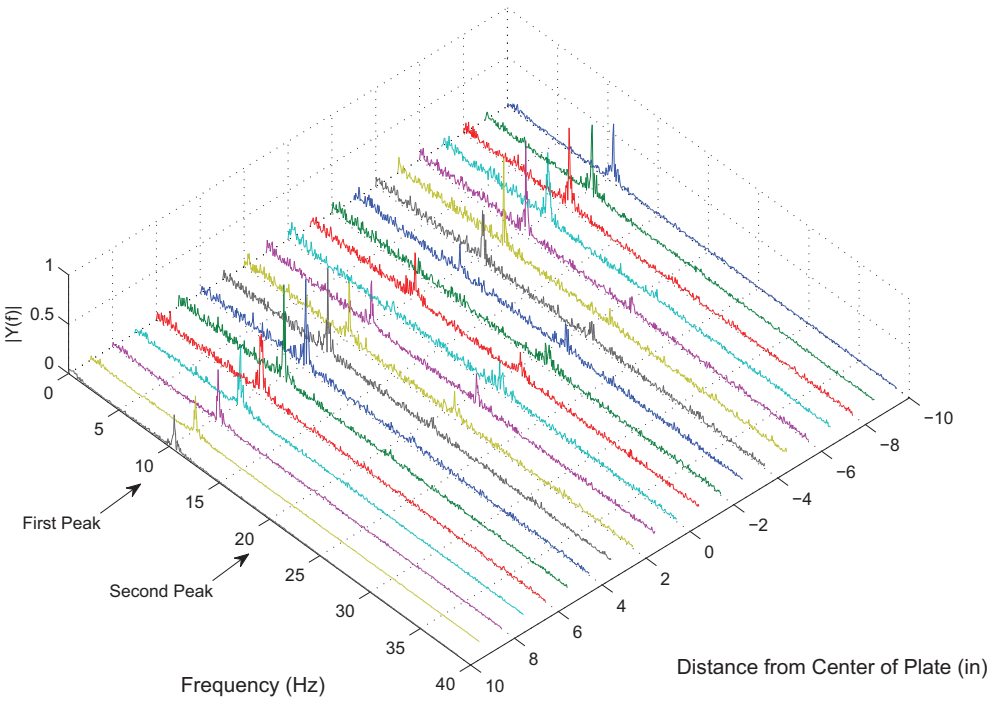

Fig. 20. Power Spectrum of Vortex Shedding

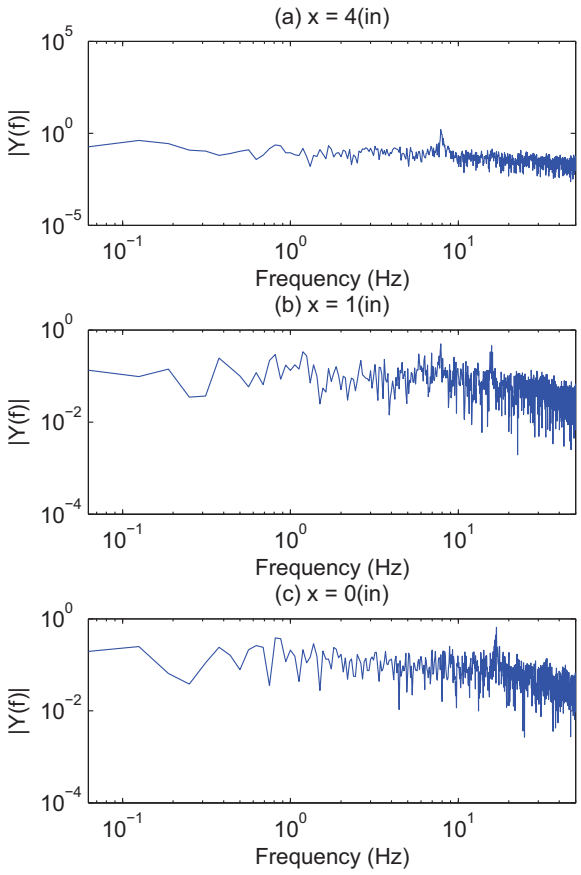

Fig. 21. Typical Power Spectrum of Vortex Shedding

the different modes are related to the spanwise point of measurement. If the point of observation is far from from the center line, there is only one peak (first peak). If the point of observation is near the center line, there may be two peaks no matter which one dominates or only the second peak. All type of spectrum are based on the spanwise location of measurement with a fixed distance from plate to hot-wire.

Comparing Figure 20(a) with (b) and (c), it is observed that the relative amplitude reflects the potential energy at each location. Figure 20(a) is the most common single peak spectrum with a first peak. The relative amplitude is highest among the three modes, which means the highest potential energy is concentrated at the point from the flow. Figure 20(c) shows the lowest amplitude and the most noises among the three modes, which indicates the counteraction of energy when two vortices are overlapped. Figure 20(b) is between the two extreme condition.

In addition to the measurement, a high speed video camera is employed to view the vortex formation region downstream of the plate. The is fixed to 240 (Hz) to capture the real time shedding video. The analog video recordings are processed by separating successive video frames into digital images. Separation of successive video frames into digital images enabled compilation of time-sequences showing vortex evolution, interaction and shedding.

The corresponding velocity at which the maximum amplitude is observed is approximately 6 m/s. The vortex shedding frequency for the stationary plate at a wind velocity of $V = 6\ m/s$ is 7.07 (Hz). The vortex formation region at a time when the vortex from the lower shear layer is fully formed. As shown in Figure 22, the shear layers and the vortex roll-up are visualized step by step on one side of the flat

plate. Figure 22 is offered primarily for the flow visualization results for the formation region behind the plate. It focuses on one side of the flat plate. These visualized images show the evolution of the vortex formation region from each side of a symmetric plate over one period (0.14 s). Images are arranged by dimensionless time (t^*) from $t^* = 1/4$ to $t^* = 1$ with increment of 1/4. Here, the dimensionless time t^* is defined as $t^* = t/T_s$, where t is the real time series and T_s is the period of vortex shedding.

C. "Lock-in" Phenomena

After obtaining the shedding characteristics for the stationary structure, LRTS (Linear Rotational Test System) is employed for the vibration tests. The vibration tests primarily focus on the "lock-in" phenomena and related conditions.

Frequencies of body vibration and vortex shedding from the oscillating body have been measured by an optical encoder and hot-wire anemometry, respectively. Signals from structural vibrations are transformed from the time domain to the frequency domain by the Fast Fourier Transformation (FFT) for each analysis. Signals from vortex shedding are also transformed by FFT to the frequency domain as been done in the stationary tests. The tests is conducted by increasing, then decreasing, a small increment of the velocity during every 24 seconds. So, the data is obtained randomly. There are 5 separate groups of tests have been conducted by the same test method. Test results shown later are a set of 5 groups of data. For each group, the velocity is increased from 3.5 m/s to approximately 22 m/s and decreased from approximately 22 m/s to 3.5 m/s. Additional several groups of tests are conducted to obtain more data in the range from 5.0 m/s to 7 m/s at which large amplitude is observed.

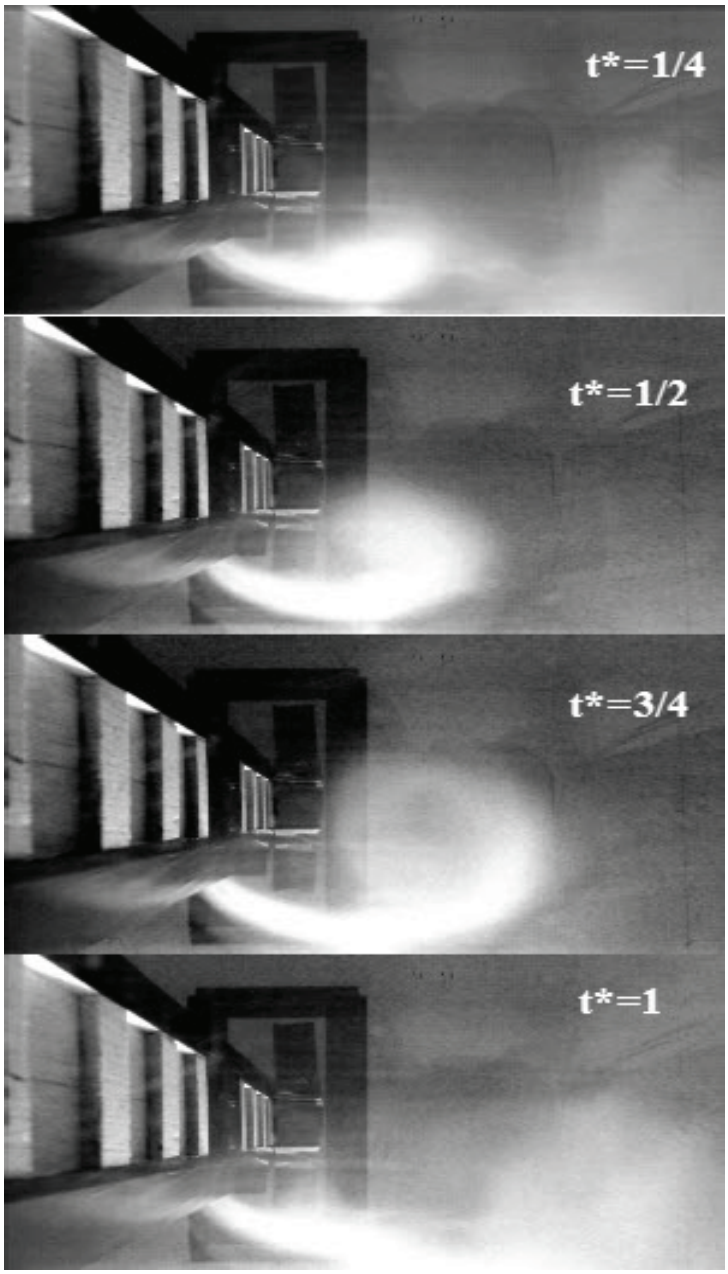

Fig. 22. Flow Pass the Stationary Flat Plate

In each series of tests, shedding frequency (f_{vs}), vibration frequency (f_{ex}), response amplitude (A_m), and velocity are recorded. The amplitude of vibration is calculated by root-mean-square. Error bars are employed to indicate the error or uncertainty in the tests. The velocity is presented as reduced velocity, defined by

$$V_r = \frac{V}{f_{vac}C} \tag{4.2}$$

where V_r is the reduced velocity, f_{vac} is the natural frequency of system in the vacuum, and C is the chord length of the plate.

Figure 23 shows the relationships between shedding frequency and Strouhal frequency when increasing velocity (Figure 23-a) and decreasing velocity (Figure 23-b). It is observed from Figure 23 that the data is almost on the reference line at which $f_{vs} = f_{st}$. This agrees with observations that for a rigid structure body, shedding frequency is closed to the Strouhal frequency with changes of flow velocity. Here, the rigid structure body means the body is a rigid member regardless of attachment to a mounting system that permit motion.

When the velocity is increased or decreased, the vortex shedding frequency is locked into the vibration frequency of the structure in a certain range, as shown in Figure 24. Figure 24-a indicates that vibration frequency and shedding frequency may lock into each other in the range from $V_r = 5$ to $V_r = 8$ for the case in which velocity is increased. Figure 24-b indicates the frequency "lock-in" range start from approximately $V_r = 5$ to $V_r = 10$ for the case in which velocity is decreased. Figure 25 and Figure 26 show the response frequency and amplitude when increasing flow velocity and decreasing flow velocity, respectively.

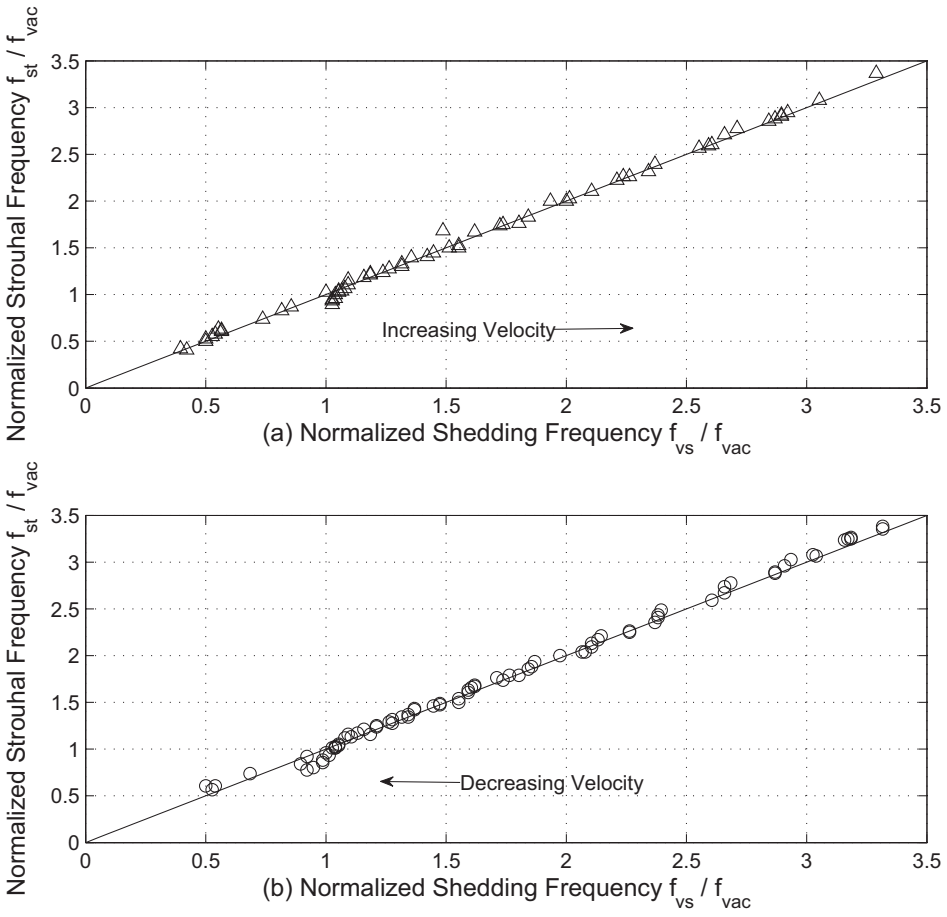

Fig. 23. Shedding Frequency versus Strouhal Frequency

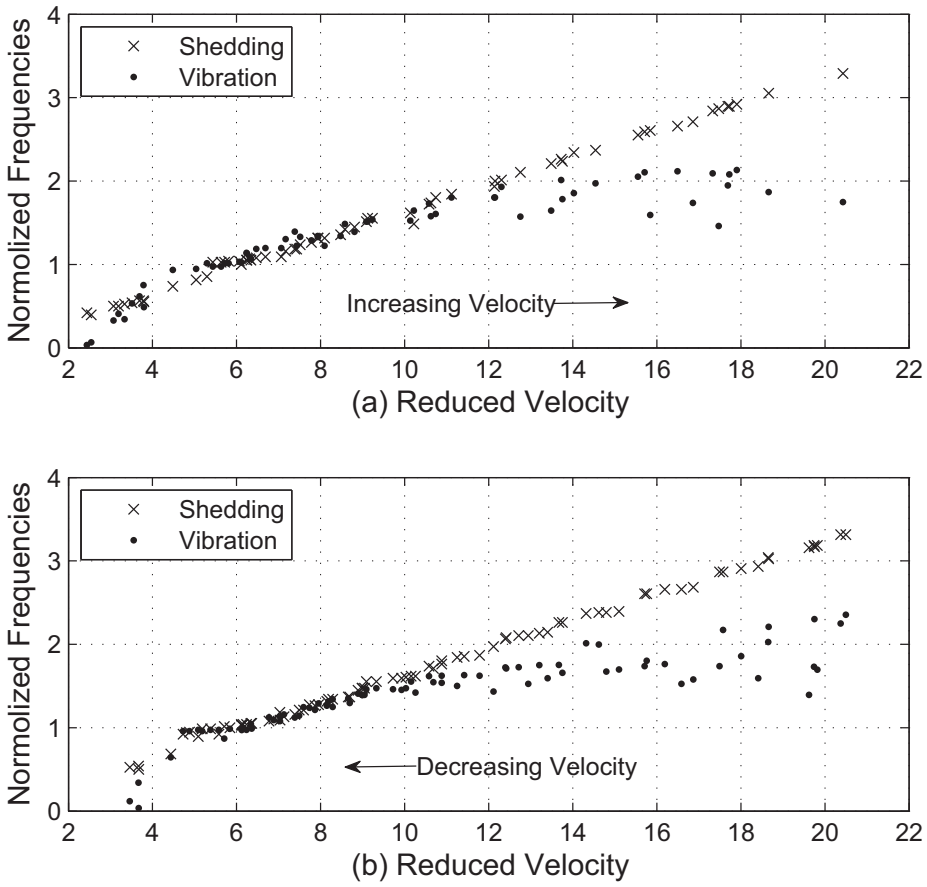

Fig. 24. Shedding Frequency versus Vibration Frequency

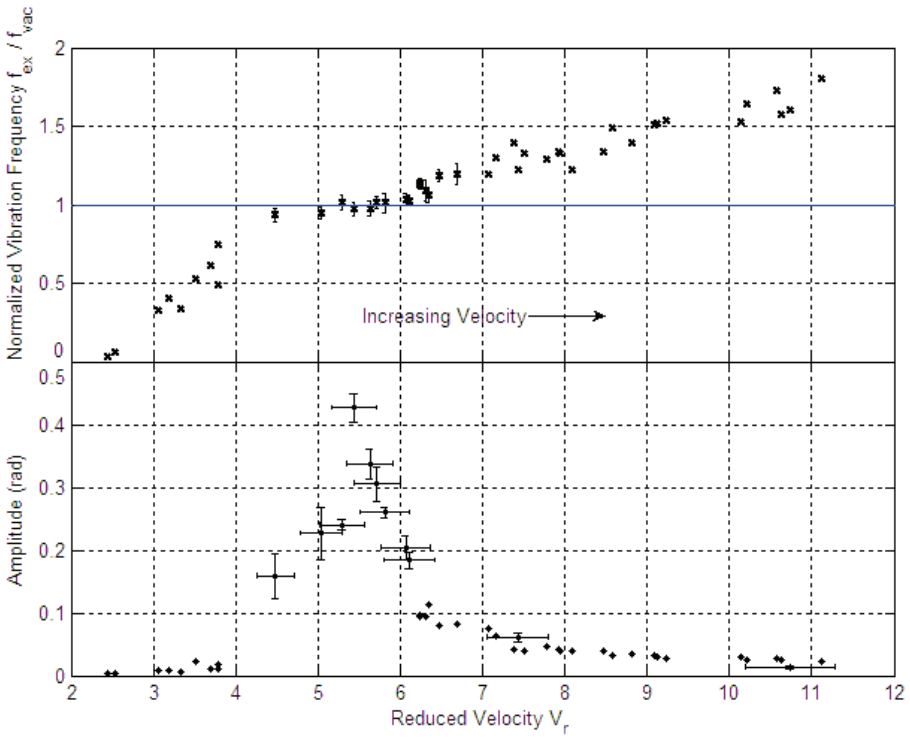

Fig. 25. Pitch Motion Amplitude and Frequency (V increase)

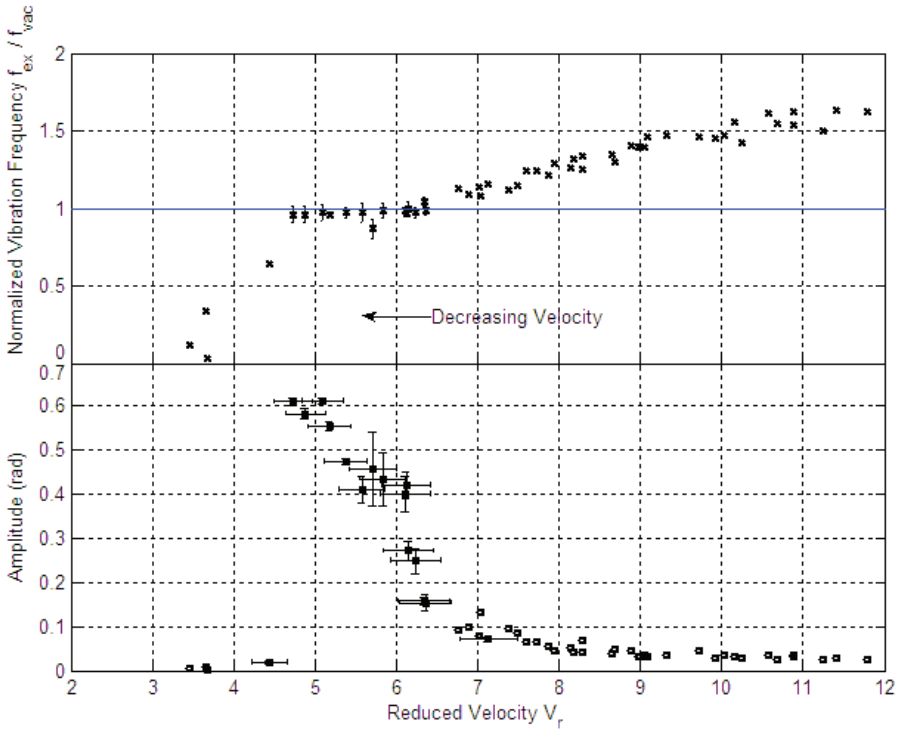

Fig. 26. Pitch Motion Amplitude and Frequency (V decrease)

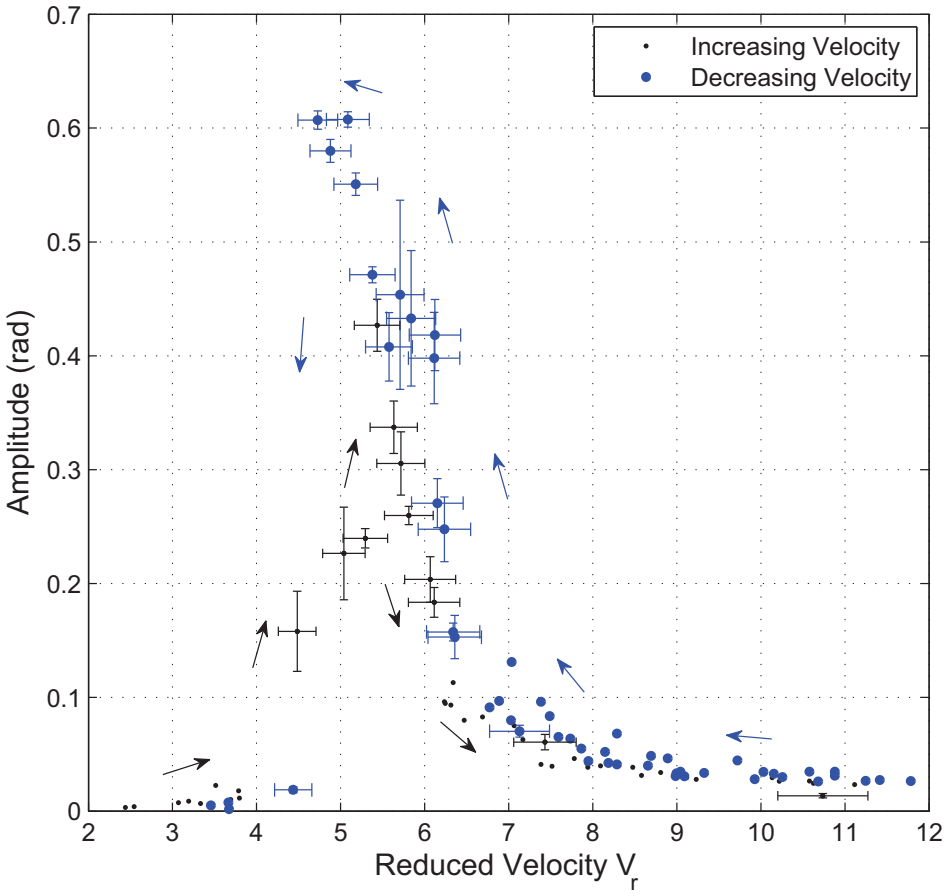

Fig. 27. Amplitude of Response as Function of Reduced Velocity

As observed in Figure 25, large-amplitude response may be clearly observed in a relative small range from $V_r = 4.9$ to $V_r = 6.5$. Figure 25 presents measurements taken as the flow velocity is increased. The maximum amplitude of oscillation reaches 0.42 rad. As shown in Figure 26, large-amplitude response is observed in the range from $V_r = 5$ to $V_r = 6.6$. Figure 26 presents measurements taken as the flow velocity is decreased. The maximum amplitude of oscillation reaches 0.61 rad, which is larger than that shown in Figure 25. It is also observed from Figure 25 and Figure 26 that large amplitude occurs when the vibration frequency of the structure is close to its natural frequency. However, compared with the bandwidth in Figure 24, large-amplitude response occurs over a narrower bandwidth. A hysteresis effect may be observed in the test due to the path (illustrated by arrow) of data collection taken as velocity is increased or as velocity is decreased, and a shift in peak amplitude of response is observed in Figure 27 due to this path.

It is also observed in the experiment that there is a sudden drop of amplitude when velocity is decreased from $V_r = 5.0$ to $V_r = 4.9$. At $V_r = 5.0$, the amplitude of oscillation reaches its maximum value. At $V_r = 4.9$, the plate appears to stop oscillation. The sudden drop of amplitude observed in the test between $V_r = 4$ to $V_r = 5$ is shown in Figure 27.

D. Summary

The Strouhal number has been measured in the stationary tests. The distribution of vortices behind the plate is provided. In the vibration tests, frequency "lock-in" and large amplitude of oscillation have been observed. The frequency "lock-in" band-

width is larger than the response amplitude bandwidth. Large amplitude may only be observed when the vibration frequency of structure is close to its natural frequency. Based upon the test results, it is concluded that the "lock-in" phenomena refers to a frequency sychronization. It does not necessarily indicate the large amplitude in its response. However, large amplitude oscillation only occurs at a narrow range at which $f_{vs} \approx f_{ex} \approx f_{vac}$. Therefore, "lock-in" may occurs when f_{vs} is not close to f_{vac}, but large amplitude may only occur near the classical resonance condition ($f_{ex} = f_{vac}$).

CHAPTER V

CONCLUSION

This research is aimed at investigating the fundamental VIV phenomena of the pitch motion for a flat plate placed in the flow. The stationary tests are conducted to find the characteristics of vortices shed from the stationary plate. The Strouhal number measured for the flat plat is 0.1647. Compared with the value $S_t = 0.145$ for flat plate(Blevins 1984), the difference may due to different shape and measured in different Reynolds number. Results from stationary tests also show the characteristics of vortices shed from the plate. A overlap of two vortices behind the plate is observed. The vibration tests are carried out to investigate the free vibration response of a elastically mounted rigid structure and its "lock-in" phenomena. The tests has been conducted in the wind tunnel within the range of $1 \times 10^4 < Re < 2 \times 10^5$.

The flow velocity is increased from 3.5 m/s to 22 m/s. "Lock-in" has been observed in the vibration tests. Associated with frequency synchronization, large amplitude of response has been observed also. A hysteresis phenomena is observed when decreasing the velocity. In the range of various flow velocities, frequency locks-into a common frequency at a relative wide range of velocity from 5 m/s to 7.5 m/s , while large amplitude may only be measured at a relative narrow range from 5.5 m/s to 6.8 m/s when increasing flow velocity. When velocity is decreased, large amplitude may be found from $V = 5.0$ m/s to $V = 6.2$ m/s, while frequency "lock-in" may be observed in a relative large range from $V = 5.0$ to $V = 6.8$.

In the frequency synchronization regime, vortex shedding frequency locks into vibration frequency of the structure with the increasing or decreasing of flow velocity

until reaching a critical flow velocity ("lock out"). In the frequency synchronization regime with large amplitude, vibration frequency and shedding frequency approach to the natural frequency of structure. Therefore, it may be concluded that "lock-in" is a distinguished phenomena in VIV. "Lock-in" is a frequency lock-in may not indicate large amplitude. Large amplitude may be found when $\frac{f_{vs}}{f_{vac}}$ approaches the neighborhood of classical resonance condition. Resonance in VIV is a "lock-in" response that corresponding to the maximum amplitude of vibration.

Further research should focus on the influence of structure and flow parameters, such as damping, stiffness and mass ratio. In addition, the two degree of freedom model including pitch-plunge coupled motion should be developed and tested.

REFERENCES

Amandolèse, X., *Hémon*, P., 2010. Vortex-induced vibration of a square cylinder in wind tunnel. Comptes Rendus Mecanique 338, 12-17.

Bearman, P.W., 1984. Vortex shedding from oscillating bluff bodies. Annual Review of Fluid Mechanics 16, 195-222.

Blackburn, H.M., Govardhan, R.N., Williamson C.H.K., 2001. A complementary numerical and physical investigation of vortex-induced vibration. Journal of Fluids and Structures 15, 481-488.

Blevins, R.D., 1977. Flow-Induced Vibration, 2nd Edition. Van Norstrand Reinhold, New York, USA.

Blevins, R.D., 1984. Applied Fluid Dynamics Handbook. Van Norstrand Reinhold, New York, USA.

Blevins, R.D., Coughran, C.S., 2009. Experiential investigation of vortex-induced vibration in one and two dimensions with variable mass, damping, and Reynolds number. Journal of Fluids Engineering 131, 1-7.

Billah, Khondokar Yusuf Razee, 1989. A Study of Vortex Induced Vibration. Ph.D. Dissertation, Princeton University, NJ.

Bishop, R.E.D., Hassan, A.Y., 1964. The lift and drag forces on a circular cylinder in a flowing fluid. Proceedings of Royal Society of London, Series A 277, 32-50, 51-75.

Botelho, dirceu Luiz Rodrigues, 1983. An Empirical Model for Vortex Induced Vibration. Ph.D. Dissertation, California Institute of Technology.

Carberry, J., Sheridan, J., Rockwell, D.O., 2001. Forces and wake modes of an oscillating cylinder. Journal of Fluids and Structures 15, 523-32.

Carberry, J., Sheridan, J., Rockwell, D.O., 2005. Controlled oscillations of a cylinder: forces and wake modes. Journal of Fluid Mechanics 538, 31-69.

Cincotta, J.J., Jones G.W., Walker R.W., 1966. Experiment investigation of wind-induced effects in two-dimensional flow with high Reynolds number. NASA Langley Research Center.

Dahl, Jason M., 2008. Vortex-induced Vibration of A Circular Cylinder with Combined In-line and Cross Motion. Ph.D. Dissertation, Massachusetts Institute of Technology.

Dowell, E.H., 1981. Non-linear oscillator models in bluff body aeroelasticity, Journal of Sound and Vibration 75, 251-264.

Facchinetti, M.L., Langre E.de, Biolley ,F., 2004. Coupling of structure and wake oscillators in vortex-induced vibration. Journal of Fluids and Structures 19, 123 -140.

Feng,C.C, 1968. The measurement of vortex induced effects in flow past stationary and oscillating circular and d-section cylinders. Master's Thesis, The University of British Columbia, Canada.

Gharib, M.R., 1999. Vortex-induced vibration, absence of lock-in and fluid force deduction. Ph.D. Dissertation, California Institute of Technology.

Govardhan,R., Williamson, C.H.K., 2000. Modes of vortex formation and frequency response of a freely vibrating cylinder. Journal of Fluid Mechanics 420, 85-130.

Gowda B.H.L., Prabhu, D.R., 1987. Interference effects on the flow-induced vibrations of a circular cylinder in side-by-side and staggered arrangement. Journal of Sound and Vibration 112, 487.

Griffin, O.M., Skop, R.A., Ramberg, S.E., 1976. Modeling of the vortex-induced oscillations of cables and bluff structures. Society for Experimental Stress Analysis Spring Meeting, Silver Spring, MD, USA.

Hartlen, R.I., Currie, R.C., 1970. Lift oscillator model of vortex-induced vibration Journal of Engineering Mechanics 96, 577-591.

Khalak ,A., Williamson, C. H. K., 1999. Motions, forces and mode transitions in vortex-induced vibrations at low mass-damping. Journal of Fluids and Structures 13, 813-851.

Lee, L., Allen, D., 2010. Vibration frequency and lock-in bandwidth of tensioned flexible cylinders experiencing vortex shedding. Journal of Fluids and Structures 26, 602-610.

Marris, A,W., 1964. A review of vortex streets, periodic wakes, and induced vibration phenomena. ASME Jounral of Basic Engineering 86, 185-196.

Moe, G., Wu, Z.J., 1990. The lift force on a cylinder vibrating in a current. ASME Journal of Offshore Mechanics and Arctic Engineering 112, 297-303.

Parkinson, Geoffery, 1989. Phenomenon and modeling of flow induced vibrations of bluff body. Progress in Aerospace Science 26, 169-224.

Protos, A., Goldschmidt, V.W., Toebes, G.H., 1968. Hydroelastic forces on bluff cylinders. ASME Journal of Basic Engineering 90, 378-386.

Reonard, A., Roshko, A., 2001. Aspect of flow-induced vibration. Journal of Fluid and Structures 15, 415-425.

Scanlan, R.H., Rosenbaum, R., 1968. Aircraft vibration and flutter. Dover, New Yo-rk, USA.

Shiels, D., Leonard, A., Roshko, A., 2001. Flow-induced vibration of a circular cylinder at limiting structural parameters. Journal of Fluids and Structures 15, 3-21.

Simiu, E., Scanlan R.H., 1986. Wind effects on structures. Van Nostrand Reinhold, New York, USA.

Skop, R.A., Griffin, R.A., 1973. Amodel for teh vortex-excited resonant response of

bluff cylinders. Journal of Sound and Vibration 27, 225-233.

Sarpkaya, T., 1978. Fluid forces on oscillating cylinders. Journal of Waterway Port Coastal and Ocean Division ASCE, WW4, 275-290.

Sarpkaya, T., 1979. Vortex-induced vibrations, a selective review. Journal of Applied Mechanics 46, 241-258.

Sarpkaya, T., 1995. Hydrodynamic damping, flow-induced oscillations, and biharmonic response. ASME Journal of Offshore Mechanics and Arctic Engieering 117, 232-238.

Sarpkaya, T., 2004. A critical review of the intrinsic nature of vortex induced vibration. Journal of Fluids and Structures 19, 389-447.

Williamson, C.H.K., Govardhan,R., 2004. Vortex-induced vibrations. Annual Review of Fluid Mechanics 36, 413-455.

Williamson, C.H.K., Roshko, A., 1988. Vortex formation in the wake of an oscillating cylinder. Journal of Fluids and Structures 2, 355-381.

Umemura, S., Yamaguchi, T., Shiraki, K., 1971. On the vibration of Cylinders caused by Karman Vortex. Bull, Japan Society of Mechanical Engineering 14, 929-936.

Van Dyke, M., 1982. An Album of Fluid Motion, 10th Edition. Parabolic Press, Stanford, CA, USA.

Vickery, B.J, Basu, R.L., 1983. Across-wind vibrations of structures of circular cross section. Part 1. Development of a model for two-dimensional conditions. Journal of Wind Engieering and Industry Aerodynamics 12, 49-73.

VITA

Yi Yang received his Bachelor of Science in Bridge Engineering from Chang'an University at Xi'an, China in 2008. He was admitted to the Civil Engineering Program at Texas A&M University in September 2008. After one year study in Texas A&M University, he entered the Aero and Fluid Dynamics Lab of the Department of Aerospace Engineering for his research under Dr. Thomas W. Strganac in September 2009. His research interests include structural dynamics, flow-induced vibration, dynamics of spacecraft, and jet propulsion.

He received his Master of Science degree in December 2010 and may pursue his Ph.D degree in areas which interest him.

He may be contacted by his email at: *yale.carl.young@gmail.com*